

University Transportation Center Initiative Final Report

Project Number:

Project Title: Vehicle Modeling for Future Generation Transportation Simulation

Project end date: 06/30/2009

Final Report submission date: 06/30/2009

Principal Investigator

Daiheng Ni, Ph.D.

Assistant Professor
Department of Civil and Environmental Engineering
University of Massachusetts Amherst

Phone: (413) 545-5408
E-mail: ni@ecs.umass.edu

May 10, 2009

Table of Contents

Executive Summary	1
Part I A Simple Dynamic Vehicle Model.....	2
I-1. Introduction.....	3
I-2. Literature Review.....	4
I-3. Development of the DIV Model	4
I-3.1. Overview of the DIV Model.....	4
I-3.2. Modeling Longitudinal Movement.....	5
Modeling Acceleration Performance	5
Modeling Braking Performance.....	6
Modeling Lateral Movement	8
I-4. DIV Model Calibration.....	9
I-5. DIV Model Validation	9
I-5.1. Test Vehicles for Validating the DIV Model	10
I-5.2. Validating Acceleration Performance	10
Evaluation of Test Results	10
I-5.3. Validating Deceleration Performance	11
Evaluation of Tests Results.....	12
I-5.4. Validating Lateral Movement.....	14
I-6. Conclusion	15
I-7. Future Directions	16
References	17
Part II A Simple Dynamic Engine Model.....	18
Notation	19
II-1. Introduction	19
II-2. Review of Existing Engine Models.....	21
II-3. Simple Mathematical Engine Models.....	23
II-3.1. Model I: Polynomial Model	23
II-3.2. Model II: Parabolic Model.....	24
II-3.3. Model III: Bernoulli Model.....	25
II-4. Validation and Comparison of the Engine Models	27
II-5. Conclusion.....	31
II-6. Appendix	31
A. A high-level comparison of engine models.....	31
B. Values for parameters in the three engine models.....	33
References	34
Part III Implementation of Vehicle Powertrain Model in Matlab Simulink	36
III-1. Modeling Vehicle Drive Chain	37
III-1.1. Forces Acting on a Vehicle.....	37
Force produced by the engine	37
Force due to Aerodynamic Drag.....	40
Net force acting on a vehicle	40
III-1.2. Vehicle Acceleration Performance	40

Engine speed	41
III-2. Implementation of Vehicle Powertrain	41
III-2.1. Data used in the Implementation	41
III-2.2. Simulink Powertrain Model Description	42
III-2.3. Simulink Powertrain Model Outputs	45

Table of Figures

Figure I-1 - Description of the coordinate system and other variables used	8
Figure I-2 - Diagonal-Plot Observed vs. DIV Simulated Results.....	11
Figure I-3 - Diagonal-Plot Observed vs. DIV Simulated Braking Distances.....	14
Figure II-1 Comparison of the three models based on 2008 Mercedes CLS engine	28
Figure II-2 Comparison of the three models based on 2006 Honda Civic engine.....	29
Figure II-3 Comparison of the three models based on 2006 Pagani Zonda engine.....	29
Figure II-4 Comparison of the three models based on 1964 Chevrolet Corvair engine.....	30
Figure II-5 Performance of the three models (left: MAPE of power, right: MAPE of torque)....	30
Figure III-1 - Key Components of an Engine's Fuel Injector System.....	37
Figure III-2 - Principle behind the engine force and the corresponding driver interaction	39
Figure III-3 Simulink model of powertrain	43
Figure III-4 Vehicle acceleration	46
Figure III-5 Vehicle speed	46
Figure III-6 Engine speed	47
Figure III-7 Vehicle displacement	47
Figure III-8 Engine performance	48

Executive Summary

Transportation systems in the 21st century are facing many critical issues including mobility and safety problems. Critical issues call for innovative technologies and solutions. Systems soon to be launched under the United States Department of Transportation (USDOT) Vehicle Infrastructure Integration (VII) Initiative are directed toward addressing these critical issues. To facilitate an understanding of the VII initiative and to assess future VII-enabled transportation systems, future generation transportation simulation tools will be required. In response to this need for simulation tools, this research proposes to develop a dynamic vehicle model as the first step toward achieving long-term VII goals. Such a model is practically unavailable but particularly needed in a VII setting because many VII-enabled vehicle and traffic control strategies work directly on vehicles and the dynamic response of these vehicles determines the effect and overall performance of the VII strategies. This project is proposed with Federal, State, and local transportation research interests in mind. In addition, this project addresses the UMass Transportation Center theme “*Improving Transportation Mobility and Safety with Innovative Technologies and Strategies*” and this research responds to a national priority by contributing to the VII initiative.

This report consists of three parts. Part I is devoted to the development of a dynamic interactive vehicle model. The model takes as inputs driver’s desired acceleration, braking, and steering and outputs longitudinal acceleration, lateral acceleration, and yaw velocity. The model requires minimal effort of calibration and the information needed to run the model is publicly available. Validation of the model against published vehicle test data reveals that the model is quite accurate in capturing vehicle dynamics. To further advance the modeling of vehicle powertrain, Part II presents a family of engine models, two of which are descriptive and one explanatory. The descriptive models represent engine power and torque as a function of engine speed by fitting empirical data, while the explanatory model relates engine speed to engine power and torque by capturing the principle of internal combustion engines. A number of measures including accuracy, computational efficiency, and accessibility are used to assess the performance of these models. Based on the assessment, a preferred model is recommended. Part III features the implementation of a vehicle powertrain model by combining models presented in the previous two parts. The implementation uses Matlab Simulink as a tool to build the powertrain model which represents vehicle as a feedback control system. The system involves the modeling of fuel supply, energy conversion, power generation, torque transmission, driving force production, acceleration performance, speed regulation, and feedback control. The powertrain model is calibrated and validated using information publicly available online. The results show that the model is capable of capture vehicle acceleration performance with reasonable accuracy.

Part I

A Simple Dynamic Vehicle Model

Recent development of inter-vehicular wireless communication technologies have motivated many innovative applications aiming at significantly increasing traffic throughput and improving highway safety. Powerful traffic simulation is an indispensable tool for developing these applications and studying their effects before large-scale deployment. One of the necessary advances to such a tool is to incorporate vehicle dynamics in traffic simulation so that the effects of improved driving strategies and the cooperation between drivers can be examined at a great level of detail. Existing dynamic vehicle models, typically developed for single vehicle applications (such as vehicle design) with high modeling fidelity, are not suited for efficient simulation of many vehicles in a traffic system. To fill the gap, we propose a simple Dynamic Interactive Vehicle (DIV) model which requires little calibration effort and computational resources. The DIV model takes as input a driver's desired level of acceleration, deceleration, and steering, and outputs vehicle dynamic responses including longitudinal and lateral accelerations, and yaw velocity.

I-1. INTRODUCTION

Recent development of the Dedicated Short Range Communication (DSRC) standard, the Vehicular Ad Hoc Networks (VANET) technologies, and more broadly the Vehicle Infrastructure Integration (VII) Initiative have motivated many innovative applications such as Cooperative Collision Warning Systems and Cooperative Highway-Vehicle Automation. These applications are promising to address national transportation priorities such as traffic congestion which causes a waste of time and fuel totaling about \$63.1 billion [1] and highway accidents which kill over 40,000 people [2] every year.

In order to facilitate the development of these applications and study their effects before large-scale deployment, a new generation traffic simulation tool is necessary for representing the new paradigm of traffic operations. For example, with VII, vehicles will be able to communicate with other vehicles as well as with the transportation infrastructure. Thus drivers will receive more timely and accurate information. Such information helps drivers to take preventive actions and supports more compact platoons without sacrificing safety. In addition, inter-vehicular DSRC allows drivers to cooperate with each other to drive more safely and efficiently. However, conventional microscopic traffic simulation tools (such as CORSIM) are unable to represent enhanced information to drivers brought about by VII and vehicle dynamic responses to improved driving strategies.

One of the dimensions to advance traffic simulation to the next generation is to incorporate vehicle dynamics so that the effects of improved driving strategies and the cooperation between drivers can be examined at a great level of detail. As an attempt toward this direction, this paper is devoted to the modeling of individual vehicle dynamics, utilizing a driver's desired acceleration, deceleration, and steering as inputs to determine vehicle dynamic responses including longitudinal acceleration, lateral acceleration, and yaw velocity. In automotive engineering, there is a wealth of literature discussing dynamic vehicle models. These models typically come with many degrees of freedom and high modeling fidelity. Typical to these models are their applications in vehicle design, handling, and stability, involving one or a few vehicles. Our interest is a dynamic vehicle model which is well suited for the simulation of a network of VII-enabled vehicles. Such an application involves large numbers of interacting and communicating vehicles, yet demands a modeling fidelity beyond the microscopic level. On this note, those vehicle models in automotive engineering are over-qualified given their complexity and high computation costs. Therefore, a Dynamic-Interactive-Vehicle (DIV) model with high computational efficiency and reasonable modeling fidelity is desirable and such a model serves as the focal point of this paper.

In the following sections, we briefly review existing efforts on representing vehicle dynamics in traffic simulation and this is followed by the development of our DIV model. After that, we present the calibration and validation process of the DIV model. At the end, we provide some concluding remarks and a few future directions.

I-2. LITERATURE REVIEW

Vehicular motion is primarily represented in traffic simulation via car-following models. There are several car-following models available today. Many of these models have a common structure which essentially has the response of the following vehicle as a function of a stimulus and a sensitivity factor. In general, the response refers to the acceleration of the following car as it tries to avoid colliding with the lead car while maintaining the driver's desired speed. The stimulus is often a function of the difference in distance and / or speed between the following and lead car. The sensitivity factor determines the weight of the response as a function of the following vehicle's speed and / or its distance behind the lead vehicle. Models with this structure that have been partly or fully implemented in traffic simulators including the Pipes model [3] and the GHR / GM model [4]. What is noteworthy here is that these models do not directly account for the acceleration / deceleration capabilities of the vehicles they are representing. Instead maximum and minimum acceleration rates of the vehicles being represented are specified by users of these models.

As researchers attempted to improve the representation of car-following behavior, models presented in [5], [6] and [7] incorporated measures designed to capture realistic acceleration performance. The work presented in [8-10] highlights the formulation and comparison of a vehicle dynamics model which is capable of successfully predicting maximum acceleration performance. The model takes into account the effect of the vehicle's engine force and other dynamic properties along with aerodynamic, rolling, and grade resistances.

The realism with which vehicle motion is represented in traffic simulation has increased over the years through the use of existing car-following and simplified vehicle dynamics models. Further improvement may incorporate vehicle braking and steering to capture vehicle longitudinal and lateral movements, rather than only modeling the longitudinal movement in existing models. Additional improvement may also occur by modeling the driver-vehicle interaction to examine the effect of enhanced information to drivers. Extending past research efforts in the modeling of vehicle dynamics will not only lead to improved understanding of traffic dynamics but also provide insights into highway design, traffic safety, more accurate estimates of vehicle emissions, and transportation forensics.

I-3. DEVELOPMENT OF THE DIV MODEL

In this section, we formulate the DIV model with the above-mentioned improvements in mind.

I-3.1. Overview of the DIV Model

The DIV model will be capable of accepting three inputs from a vehicle driver: throttle position, brake pedal position, and the steering angle. The model will relate each input to a particular driver's desire and represent these various desires on a scale of 0 to 1 for the throttle and brake positions, and -1 to +1 for the steering angle. Each of these parameters will then interact with their corresponding mechanisms to produce motion. The following sections will present how

DIV model treats the various components of a vehicle in order to faithfully capture its motion. These components include the engine, the braking system and the steering mechanism. Details of how the DIV model will account for effects due to rolling resistance, air resistance and gravity will also be presented in the following sections.

I-3.2. Modeling Longitudinal Movement

Forces in the longitudinal direction of the DIV model include the forces due to the engine and the braking system, rolling and aerodynamic resistances, and the force due to gravity. The equation of motion for such a vehicle can be derived by using Newton second law of motion:

$$\sum F = ma = \frac{W}{g}a = F_e - F_b - R_a - R_r - R_g \quad (1)$$

Where:

W	=	weight of the vehicle (kg)
g	=	acceleration due to gravity (m/s ²)
F_e	=	tractive force produced by the engine (N)
F_b	=	force produce by the brake (N)
R_a	=	aerodynamic Resistance (N)
R_r	=	rolling resistance (N)
R_g	=	grade resistance (N)

Modeling Acceleration Performance

An engine plays an important role in vehicle acceleration performance. Here we adopt the engine model in [11] which is briefly described below. The mass of air flowing into the engine's cylinders, m_a , is equal to

$$m_a = \rho_2 \cdot V_a \quad (2)$$

where:

ρ_2	-	density of the air in the combustion chamber (kg/m ³)
V_a	-	Total volume of the air in the combustion chamber of the engine (m ³)

However ρ_2 and V_a need to be calculated first. The volume of air in all the combustion chambers of the engine, V_a , is essentially the product of the engine's displacement and its speed; resulting in:

$$V_a = V_e \cdot \frac{1}{2} \cdot \frac{\omega}{2\pi} \quad (3)$$

where:

V_e - engine displacement (m³)
 ω - engine speed (rad/s)

As for the density of air in the combustion chamber, ρ_2 , it was calculated based on Bernoulli's Principle, which in essence states that an increase in the speed of a fluid results in a decrease in the pressure or gravitational energy experienced by that fluid as long as there is no work being done on the fluid. In calculating ρ_2 , the cross-sectional areas of the inlet manifold and the opened throttle, along with their respective air pressure and densities were used. Therefore, after several iterations:

$$\rho_2 = \rho_0 - \frac{\rho_0^2 V_a^2}{2 A_0^2 p_0} \left(\frac{1}{\theta} + \frac{A_0^2}{A_2^2} - 2 \right) \quad (4)$$

where:

A_0 - cross-sectional area of the inlet manifold (m²)
 A_2 - cross-sectional area of the inlet valve (m²)
 ρ_0 - density of air flow before the throttle (kg/m³)
 p_0 - air pressure before the throttle (N/m²)
 θ - throttle position (percent of throttle opening)

After computing the mass of air being taken into to the engine block the corresponding amount of fuel may be estimated using the Stoichiometric air-fuel ratio (λ) for gasoline, which is 6.8%. Having a value for the amount of fuel entering into the engine, the amount of power generated by this quantity of fuel is determined by using the energy fuel density of gasoline, E_f , which is 46.9 MJ/kg. It is known that the efficiency of an internal combustion engine, η , is not 100% and are reflected in subsequent calculations. The effective power, P_{eff} , delivered to the vehicle's power-train mechanism is defined as:

$$P_{eff} = \eta \lambda E_f m_a \quad (5)$$

With the effective power calculated the effective torque, T_{eff} , delivered to the wheels of the vehicle can be determined with the following relationship:

$$T_{eff} = \frac{P_{eff}}{\omega} \quad (6)$$

Using the effective torque being delivered to the wheel, the effective engine force, F_e , produced by the engine to promote vehicle motion can therefore be calculated with the aid of the appropriate final transmission gear ratio, N_{ft} , and wheel radius, r .

$$F_e = \frac{T_{eff} \cdot N_{ft}}{r} \quad (7)$$

Modeling Braking Performance

The brake system will be represented by equating the force applied to the brake pedal by the driver to the corresponding deceleration of the vehicle. This means of representing the braking

ability of a vehicle is as a result of the work presented in [12]. The objective of this study was to define the brake characteristics within the space bounded by the relationship between brake pedal force and vehicle deceleration, which will lead to acceptable driver-vehicle performance. In essence, this study determined ergonomic properties for brake pedals that would give drivers the most effective control [13]. Therefore, using the results from this study, the DIV model will be able to not only account for the braking performance of the vehicle but also the manner in which the driver interacts with the brake system.

The results of the aforementioned study include several linear relationships which describe the force being applied to the brake pedal and the rate of deceleration of the vehicle. From these relationships, the DIV model will use the proportionality constant to provide optimal pedal force gain. This proportionality constant, 0.021 g/lb, corresponds to maximum deceleration rate through minimal pedal force. Using this proportionality constant, the following formulation will be used in the DIV model to represent the brake system of a vehicle and the driver's interaction with that system.

$$F_b = d_{brk} \times p_f \times W \quad (8)$$

where:

$$\begin{aligned} F_b &= \text{Brake Force (N)} \\ D_{brk} &= \text{driver's desire to brake (0-1)} \\ p_f &= \text{pedal-force gain coefficient} \end{aligned}$$

Aerodynamic drag is another force that retards the motion of a vehicle. This force is dependent on atmospheric conditions, the frontal area of the vehicle, A_f , and the velocity at which the vehicle is traveling relative to the wind, V_r . The equation below further describes aerodynamic drag, [14]:

$$R_a = \frac{\rho}{2} C_D A_f V_r^2 \quad (9)$$

where:

$$\begin{aligned} \rho &= \text{Mass density of the air (0.07651 lb/ft}^3\text{- performance test condition)} \\ C_D &= \text{Coefficient of aerodynamic resistance} \end{aligned}$$

The force due to gravity is mainly experienced when the vehicle is on an incline. The force due to gravity that is acting on the vehicle is calculated by, [13]:

$$F_g = \pm W \sin \theta \cong W \theta \quad (10)$$

where:

$$\theta = \text{Grade of the incline in radians}$$

Modeling Lateral Movement

The structure used to represent the movement of the DIV model in the X-Y plane was adapted from [15], which included the formulation a kinematics and a dynamic framework to model a vehicle's motion in a two-dimensional space. The kinematics framework that was presented in the aforementioned manuscript was chosen for the DIV model for two primary reasons: 1) all the pertinent dynamic properties of the vehicle were already accounted by other means in the DIV model, and 2) the ease of use with accurate X-Y position representation.

At the base of the kinematics framework for the 2-D representation of vehicle motion is the treatment of the vehicle as a non-homonymic system, which is a system that does not guarantee return to its original position, even if its original configuration is reached. Along with the non-homonymic treatment of the vehicle, non-homonymic constraints, which are related to the velocity of the vehicle, are held under the assumption that there is no slippage at the wheels during a turn. The assumption that there is no slippage at the wheels is predominantly applicable to instances of high speed cornering, as wheel slippage of low speeds is negligible. The general form of the non-holonomic constraint maybe represented as:

$$\dot{x} \sin(\varphi) - \dot{y} \cos(\varphi) = 0 \quad (11)$$

Where \dot{x} and \dot{y} represent the velocities in the x and the y directions of the vehicle coordinate system and δ is the vehicle orientation with respect to the global X-Y coordinate system. See Figure I-1 for an illustration of the coordinate system being used and also the definition of variables that will be used in the development of the DIV model.

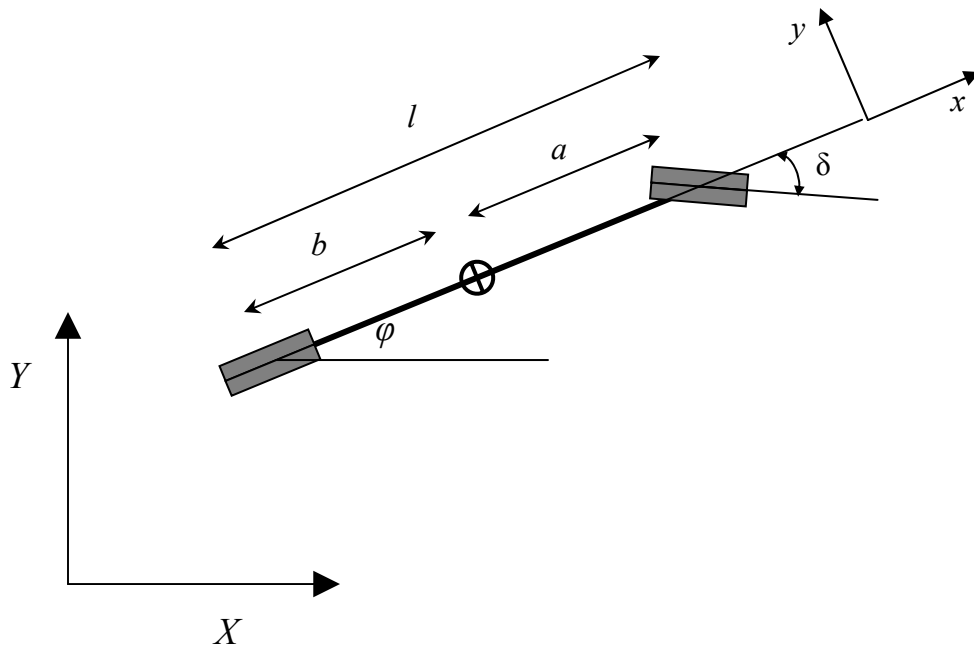


Figure I-1 - Description of the coordinate system and other variables used

After a few more iterations of **Eq. 11** the velocity of the center of gravity with respect to the global coordinate system is defined as:

$$\begin{aligned} \dot{X} &= \dot{x} \cos(\varphi) - \dot{y} \sin(\varphi) \\ \dot{Y} &= \dot{x} \sin(\varphi) + \dot{y} \cos(\varphi) \end{aligned} \quad (12, 13)$$

Having **Eq. 12** and **Eq. 13**, the global position of the vehicle can now be determined. However, before these equations can be used lateral velocity, y' , has to be defined. The definition of the Ackerman angle, δ , also has to be introduced as this is the parameter that is responsible for change the orientation of the vehicle.

$$\dot{y} = \dot{\phi} b \quad (14, 15)$$

And
$$\dot{\phi} = \frac{\tan(\delta)}{l} \dot{x}$$

$$\delta = d_{turn} \cdot \frac{\pi \cdot lck_lck}{S_{ratio}} \quad (16)$$

where:

- d_{turn} - Driver's desire to turn (-1 to +1)
- lck_lck - # of steering wheel revolutions from one lock to the next
- S_{ratio} - Steer ratio (ratio of radians dialed to Ackerman angle)

I-4. DIV MODEL CALIBRATION

A key feature of the DIV model is that it is meant to be easily calibrated. The calibration process of the DIV model will entail the user providing the model with few performance specifications of the vehicle being modeled. These specifications will be assessable as they are available to the public via car manufactures and various organizations that offer tools to research a myriad vehicles, for example Cars.com. The vehicle performance specifications that the DIV model requires include: aerodynamic resistance coefficient, engine displacement, gear ratios, steer ratio, and the vehicle dimensions.

In addition to these specifications, the model also has a few variables relating to the environment that impact vehicle motion, including wind speed and gradient of the roadway. Once the values of the vehicle performance specification and the various values describing the surrounding environment are entered into the DIV model, it will be able to replicate the motion of the vehicle.

I-5. DIV MODEL VALIDATION

In validating the DIV model, three standard performance tests were used to determine whether or not the DIV model is capable of successfully replicating the movement of the vehicle. These tests are typically conducted on vehicles to determine their capabilities of accelerating, braking, and handling. To test vehicle acceleration, the time for a vehicle to go from rest to 97 kph (60 mph) is recorded, as well as the time it takes a vehicle to cover a distance of 402 m (¼ mile). The Federal Motor Carrier Safety Administration (FMCSA) dictates maximum allowable stopping distances from various speeds that all vehicle manufacturers must satisfy, standardizing vehicle braking. And finally, to measure how well a vehicle handles, the diameter of the circle

scribed by the vehicle's outer front wheel is recorded, after the maximum steering angle has been dialed.

I-5.1. Test Vehicles for Validating the DIV Model

To increase the applicability of the DIV model, passenger cars were chosen, representing approximately 58% of the registered passenger vehicles in the United States in 2004 [16]. Therefore, upon successful validation of the DIV model with the use of passenger cars, the DIV model will be capable of representing the majority of vehicles of today's roadways. Three different types of passenger cars were used in this validation process – a sports car - 2006 Porsche Cayman S, a large passenger car - 2006 Ford Fusion Sedan SE, and a small passenger car - 2006 Honda Civic Coupe EX.

I-5.2. Validating Acceleration Performance

As previously mentioned, the tests chosen to verify how well the DIV model replicates the acceleration performance of an automobile are the 0 – 97 kph (0 – 60 mph) test and the 402 m (¼ mile) test. In these tests, the driver of the vehicle opens the throttle body to its maximum position and the time it takes the vehicle to get from rest to 97 kph (60 mph), as well as the time taken for the vehicle to cover a distance of a 402 m (¼ mile) are recorded. The DIV model simulated these tests and its results were compared to the published results for the test vehicles of similar tests. Published results for the various tests were obtained from [17]. The comparisons of test results are presented in Table I-1.

Table I-1 - Comparison of Acceleration Performance DIV Model vs. Real Vehicles

Tests	Porsche Cayman S			Ford Fusion			Honda Civic		
	<i>Obs.</i> <i>(sec)</i>	<i>DIV</i> <i>(sec)</i>	<i>Error</i> <i>(%)</i>	<i>Obs.</i> <i>(sec)</i>	<i>DIV</i> <i>(sec)</i>	<i>Error</i> <i>(%)</i>	<i>Obs.</i> <i>(sec)</i>	<i>DIV</i> <i>(sec)</i>	<i>Error</i> <i>(%)</i>
0-97 kph (0-60 mph)	5.15	4.98	3.30	6.89	6.78	1.60	7.84	7.74	1.28
402 m (¼ mile)	13.67	13.20	3.44	15.47	15.05	2.71	16.08	15.89	1.18

Evaluation of Test Results

The absolute percentage error between the observed results and that of the DIV model provides a means of quantitatively validating the DIV model. For the purpose of this paper, an absolute percentage no greater than 5% between the observed results and that of the DIV model represents a successful attempt by the DIV model in replicating the acceleration performance of a *real* vehicle. As seen from the above table the absolute percentage error ranges from 1.60% to

3.44%, signifying that fact that the DIV model is successful at replicating an automobile's acceleration performance.

To further highlight the validity of the DIV model, as it attempts to represent the acceleration performance of an automobile, a diagonal plot was created. The diagonal plot provides a means of qualitatively evaluating how well the DIV model replicated acceleration performances. In essence, for the diagonal plot, if the simulated mechanism, in this case the DIV model, replicated the observed results then the ideal fit will be a 45° line. As seen from Figure I-2 this is almost the case, once again proving the validity for the DIV model when replicating acceleration performance. [18]

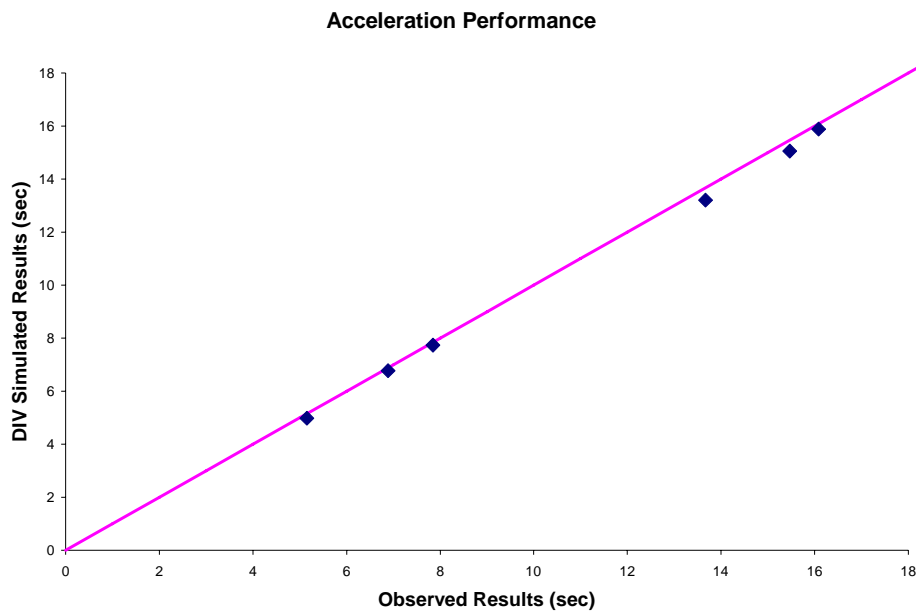


Figure I-2 - Diagonal-Plot Observed vs. DIV Simulated Results

I-5.3. Validating Deceleration Performance

Due to the complexity of the braking system and the various ways of measuring braking performance the DIV model's braking capabilities will be validated by comparing its performance to the safety standards set by the Federal Motor Carrier Safety Administration. The braking performance of the DIV model will be compared to Part 571 of the Federal Motor Vehicle Safety Standards – Standard No. 105, which describes the requirements for Hydraulic and Electric Brake Systems. [19]

There are four effectiveness tests geared toward ensuring safe braking performance.

Effectiveness Test #1 – a small vehicle / passenger car, with pre-burnished brakes, should be able to come to rest from 48 kph (30 mph) and 97 kph (60 mph) within 17 m (57 ft) and 66 m (216 ft) respectively.

Effectiveness Test #2 – a passenger car should be able to rest from speeds of 48 kph (30 mph), 97 kph (60 mph) and 129 kph (80 mph) within 16 m (54 ft), 62 m (204 ft) and 117m (383 ft) respectively.

Effectiveness Test #3 – a lightly loaded passenger car should be able to come to rest from 97 kph (60 mph) within 59 m (194 feet).

Effectiveness Test #4 – a passenger car should be able to come to rest from speeds of 48 kph (30 mph), 97 kph (60 mph), 129 kph (80 mph) and 161 kph (100 mph) within distances of 17 m (57 ft), 66 m (216 ft), 123 (405 ft), and 205 m (673 ft) respectively.

Note that when referring to brakes being pre-burnished and burnished, the DIV model will not account for the difference between the two. This largely due to the complexity in treating the two stages of how worn the brakes are and the lack added fidelity that would be gained upon including the effects of pre-burnished and burnished brakes. Another point of clarification is the definition of a lightly loaded vehicle. According the Federal Motor Carrier Safety Administration a lightly loaded vehicle is the unloaded vehicle weight plus 181 kg (400 lbs).

Evaluation of Tests Results

In carrying out the various effectiveness tests on the DIV model, after the speed, specified by the test, is reached the driver applies maximum brake force. The stopping distance is then calculated based on the distance travel between the times the driver applies the brake to when the car comes to rest. In testing the braking performance of the DIV model, the four effectiveness tests were conducted on the DIV model's representation of the three test vehicles and the results summarized in Table I-2.

It is important to clarify the meaning of the numbers in Standard No. 105 in order to evaluate the success of a model in terms of its ability to replicate the braking performance of real vehicles. Note that these numbers are *upper bounds* (i.e. the maximum allowable distances) set by the Federal Motor Carrier Safety Administration to ensure that car makers produce braking systems that can bring cars to rest from a series of initial conditions within a specified distance after the driver has applied the brake. Therefore, a model is successful if it produces a stopping distance that is less than or no greater than 5% of the stopping distance specified for a particular effectiveness test.

Table I-2 - Braking Performance Results and Analysis

Braking Performance	Standard No. 105	DIV	Error	Success
	Stop Dist. m (ft)	Stop Dist. (ft)	%	
Porsche Cayman S				
Effectiveness Test #1	17 (57)	17.12 (56.18)	-1.4	✓
	66 (216)	60.97 (200.04)	-7.4	✓
Effectiveness Test #2	16 (54)	17.12 (56.18)	4.0	✓
	62 (204)	60.97 (200.04)	-1.9	✓
	117 (383)	99.06 (325)	-15.1	✓
Effectiveness Test #3	59 (194)	60.92 (199.87)	3.0	✓
Effectiveness Test #4	17 (57)	17.12 (56.18)	-1.4	✓
	66 (216)	60.97 (200.04)	-7.4	✓
	123 (405)	99.06 (325)	-19.8	✓
	205 (673)	143.17 (469.72)	-30.2	✓
Ford Fusion				
Effectiveness Test #1	17 (57)	18.79 (61.67)	8.2	✗
	66 (216)	64.87 (212.83)	-1.5	✓
Effectiveness Test #2	16 (54)	18.79 (61.67)	14.2	✗
	62 (204)	64.87 (212.83)	4.3	✓
	117 (383)	103.70 (340.23)	-11.2	✓
Effectiveness Test #3	59 (194)	64.91 (212.97)	9.8	✗
Effectiveness Test #4	17 (57)	18.79 (61.67)	8.2	✗
	66 (216)	64.87 (212.83)	-1.5	✓
	123 (405)	103.70 (340.23)	-16.0	✓
	205 (673)	147.33 (483.35)	-28.2	✓
Honda Civic				
Effectiveness Test #1	17 (57)	68.06 (68.06)	19.4	✗
	66 (216)	72.37 (237.44)	9.9	✗
Effectiveness Test #2	16 (54)	68.06 (68.06)	26.0	✗
	62 (204)	72.37 (237.44)	16.4	✗
	117 (383)	116.59 (382.50)	-0.1	✓
Effectiveness Test #3	59 (194)	71.25 (233.77)	20.5	✗
Effectiveness Test #4	17 (57)	68.06 (68.06)	19.4	✗
	66 (216)	72.37 (237.44)	9.9	✗
	123 (405)	116.59 (382.50)	-5.6	✓
	205 (673)	156.89 (514.74)	-23.5	✓

In Table I-2, and are used to indicate whether or not the DIV model was successful at representing the braking performance of a particular vehicle during a specific effectiveness test. The represents a successful replication of the braking performance and the represents a failure. The above evaluation of the test results was a quantitative means of validating the model. For a qualitative evaluation of the model Figure I-3 illustrates a diagonal plot of the Standard No. 105 upper bounds versus the braking performance results from the DIV model.

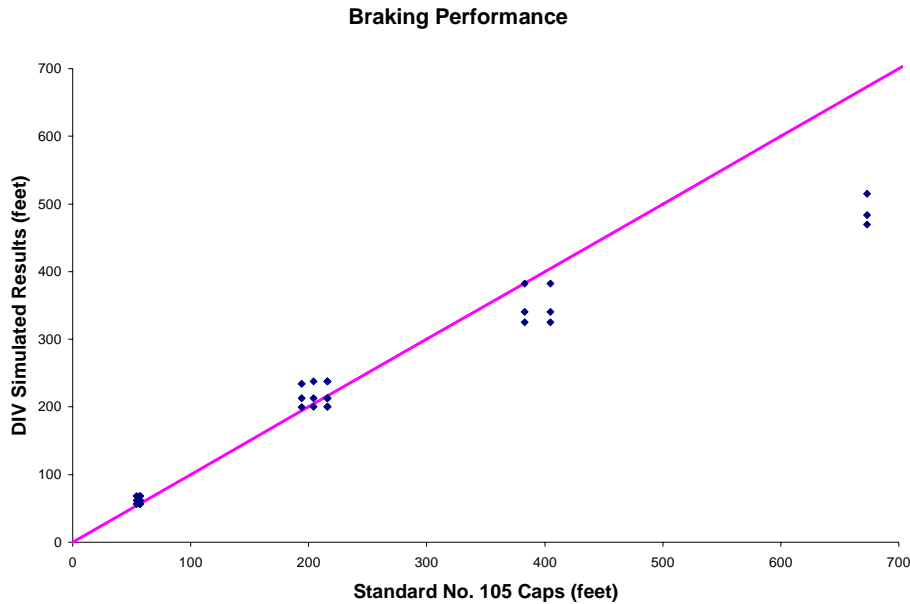


Figure I-3 - Diagonal-Plot Observed vs. DIV Simulated Braking Distances

As discussed above, points above the 45° line in this diagonal plot represent instances where the DIV model failed to produce stopping distances that are within the standards set by the FMCSA, while points on or below the line represents instances of success.

Examining both the quantitative and qualitative evaluations of the test results of the DIV model's ability to replicate braking performance, one will notice that in light of the several instances where the DIV failed to produce stopping distances under the aforementioned boundaries, the model still performs relatively well. This level of success in the midst of the instances of failure provides motivation for additional research, to correct the problems that may lie in the DIV model.

I-5.4. Validating Lateral Movement

To illustrate this validation process the 2006 Porsche Cayman S lateral movement test is presented. The turning circle as defined by Road and Track Magazine is the circle that is scribed by the outside front tire when the maximum steering lock dialed in. The measurement that is often used to represent the turning circle of a given automobile is the diameter of that circle.

According to the manufacture’s specifications, the 2006 Porsche Cayman S, with a steering ratio of 15.5:1, scribes a turning circle with an approximate diameter of 11.1 m (36.4 ft).

Using all the specifications of the Porsche Cayman S in the DIV model and dialing the maximum steering lock, the diameter of the turning circle is approximately 11.23 m (36.87 ft). The diameter determined by the DIV model has to be converted from the diameter of the circle scribed by the center of gravity 8.58 m (28.15 ft.) to the diameter of the circle scribed by the outer front wheel of the vehicle. To do this, the distance from the center of gravity to the center of the front axle is calculated, doubled 2.66 m (8.72 ft.) and then added to the diameter of the circle scribed by the center of gravity.

Similar procedures were conducted to determine how well the DIV model is capable of reproducing the turning circles of the other two test vehicles. The DIV model’s results of the diameters of the vehicles’ turning circles and the corresponding absolute percentage errors are presented in Table I-3.

Table I-3- Diameter of Turning Circle - DIV Model vs. Real Vehicles

Turning Circle	Porsche Cayman S			Ford Fusion			Honda Civic		
	<i>Obs.</i> (m)	<i>DIV</i> (m)	<i>Error</i> (%)	<i>Obs.</i> (m)	<i>DIV</i> (m)	<i>Error</i> (%)	<i>Obs.</i> (m)	<i>DIV</i> (m)	<i>Error</i> (%)
Diameter	11.09	11.24	1.29	12.19	12.86	5.47	10.79	10.29	4.60

In terms of validating this aspect of the DIV model, a successful representation of the lateral movement of an automobile is had when the absolute percentage error in the DIV model’s output of the diameter of a turning circle is no greater 5% of the published corresponding value. Given the percentage error in the above table, it can be deduced that the DIV model demonstrate a rather high level of success when replicating a vehicle’s lateral movement.

I-6. CONCLUSION

The DIV model is a simple and computationally affordable vehicle dynamics model which is able to represent vehicle motion with a reasonable fidelity. Upon validating the DIV model, its capabilities of replicating three sets of performance test results for three passenger cars were demonstrated. The three performance tests measure how well a vehicle accelerates, brakes, and turns.

The acceleration test included a measure of how long it takes a vehicle to accelerate from rest to 97 kph (60 mph) and also how long it takes a vehicle to cover 402 m (¼ mile). The DIV model output times whose absolute percentage errors are no greater than 3.5% of the observed values of the three test vehicles - well within the 5% range criteria used to represent successful replication

of acceleration performance. As for the brake performance test, the DIV model outputs the required distances to bring a vehicle to rest from particular speeds. These values of stopping distances were compared to a series of standards (upper bounds) set by the Federal Motor Carrier Safety Administration (FMCSA). In several instances the DIV model was able to output distances within the limits set by the FMCSA; however, there are few instances in which the DIV model's output exceeded the standards. The Porsche Cayman representation was the most successful, while the Honda Civic representation was the least successful. In the performance test to determine how well the DIV model represents lateral movement, we calculated the diameter of the circle scribed by the outer front wheel of the vehicle after the maximum steering angle was dialed. The absolute percentage error between the DIV model's results and those measured from real passenger cars were no more than 5.5%.

The DIV model realistically replicates the two-dimensional movement of an automobile, while allowing interactions with both the driver and the road. In addition, due to its simple mathematical representation, the DIV model is very computationally efficient involving little calibration efforts.

I-7. FUTURE DIRECTIONS

Future directions of this research effort can be focused on three specific areas: the mathematical representation of a vehicle's braking system, the comprehensive treatment of the lateral movement of a vehicle and the validation procedure in determine how well the vehicle model is capable of representing vehicle dynamics.

The Braking System: Currently, the DIV model treats the brake system of a vehicle according to the result from a Driver-Vehicle Braking Performance study conducted in 1970 [12]. Not only is this study due for an update given the advances in the brake technology used on today's vehicles, but also this treatment of the braking system is not vehicle specific. The next step for the DIV model in representing the brake system of a vehicle is to utilize simplified mathematical representations of how a driver places her foot on the brake pedal and produce a force on the wheels, retarding the motion of a vehicle.

Lateral Vehicle Movement: The DIV does a relatively good job of representing the lateral movement of a vehicle at low speeds. When representing a vehicle's lateral motion the DIV model does not account for slippage at the tire-road interface. At low speeds slippage is negligible and does not affect the motion of a vehicle. But at a high speeds, tremendous slippage can occur and greatly influences the motion of a vehicle. Therefore the next step for the DIV model is to account for slippage at the tire-road interface.

Validation Procedure: The current performance tests involved in the validation procedure only test performances with maximum driver input, i.e. maximum gas and brake pedal displacement and maximum steering angle. The next step would be to conduct performance test on both a real vehicle and the DIV model where maximum driver input is rare.

REFERENCES

1. TTI, *2005 Urban Mobility Study*. 2005.
2. BTS, *National Transportation Statistics 2006*. 2006.
3. Pipes, L.A., *An Operational Analysis of Traffic Dynamics*. Journal of Applied Physics, 1953. **24**(3): p. 274-281.
4. Gazis, D.C., R. Herman, and R.B. Potts, *Car-Following Theory of Steady-State Traffic Flow*. Operations Research 1959. **7**(6).
5. Gipps, P.G., *A Behavioural Car-Following Model for Computer Simulation*. Transportation Research Part B: Methodological, 1981. **15B**(2): p. 105-111.
6. Benekohal, R.F. and J. Treiterer, *CARSIM: Car-Following Model for Simulation of Traffic in Normal Stop-and-Go Conditions*. Transportation Research Record, 1988. **1194**: p. 99-111.
7. Helbing, D., et al., *Micro- and Macro- Simulation of Freeway Traffic*. Mathematical and Computer Modelling, 2002. **35**(5/6): p. 517-547.
8. Rakha, H. and I. Lucic, *Variable Power Vehicle Dynamics Model for Estimating Truck Acceleration*. Journal of Transportation Engineering, 2002. **128**(5): p. 412-419.
9. Rakha, H., et al., *Vehicle Dynamics Model for Predicting Maximum Truck Acceleration Levels*. Journal of Transportation Engineering, 2001. **127**(5): p. 418-425.
10. Rakha, H., M. Snare, and F. Dion, *Vehicle Dynamics Model for Estimating Maximum Light Duty Vehicle Acceleration Levels*, in *Paper submitted for Presentation and Publication at the 83rd Transportation Research Board Meeting*. 2003, Virginia Tech Transportation Institute: Virginia. p. 22.
11. Ni, D. and D. Henclewood, *Simple Engine Models for VII-Enabled In-Vehicle Applications*. Accepted for publication by IEEE Transactions on Vehicular Technology, 2008.
12. Mortimer, R.G., et al., *Brake Force Requirement Study: Driver-Vehicle Braking Performance as a Function of Brake System Design Variables*. 1970, University of Michigan: Ann Arbor, Michigan. p. 32.
13. Gillespie, T.D., *Fundamentals of Vehicle Dynamics*. 1992, Warrendale. PA: Society of Automotive Engineers, Inc. 495.
14. Wong, J.Y., *Theory of Ground Vehicles*. Third ed. 2001, New York: John Wiley and Sons, Inc. 528.
15. Moret, E.N., *Dynamic Modeling and Control of a Car-Like Robot*, in *Electrical Engineering*. 2003, Virginia Polytechnic Institute and State University: Blacksburg, VA. p. 88.
16. BTS, *Number of U.S. Aircraft, Vehicles, Vessels, and Other Conveyances*. 2004, U.S. Department of Transportation (US DOT) Washington, DC.
17. Cars.com. *Cars.com Home Page*. 2007 [July 8, 2007].
18. Ni, D., et al., *Systematic Approach for Validating Traffic Simulation Models*. Transportation Research Record 2004. **1876**: p. 12.
19. FMCSA, F.M.C.S.A. *Part 571: Federal Motor Vehicle Safety Standards: Standard No. 105; Hydraulic and Electric Brake Systems* 2005 [cited June 5, 2007]; http://www.fmcsa.dot.gov/rules-regulations/administration/fmcsr/fmcsrruletext.asp?rule_toc=777§ion=571.105§ion_toc=2072].

Part II

A Simple Dynamic Engine Model

Engine modeling plays an important role in many transportation applications such as interactive highway safety design, mobile source emission estimation, vehicle infrastructure integration, and future generation transportation simulation. Though many engine models have been developed in the past, an appropriate model suited for transportation applications is practically unavailable. This is because the nature of transportation applications sets forth special criteria on such a model. These criteria include reasonable accuracy, computational efficiency, model accessibility (i.e. the involvement of proprietary parameters and variables which are difficult to measure). This paper presents three simple engine models with one existing and two being developed by the authors. Model evaluation based on empirical validation suggests that one of the models appears promising in terms of all the criteria.

NOTATION

Symbol	Definition	Unit
P	Engine power. P_{\max} is the peak engine power	W
Γ	Engine torque. Γ_{\max} is the peak engine torque	$N\cdot m$
ω	Engine speed. ω_p and ω_t are engine speeds when power and torque peak respectively.	rad/s
V_e	Engine displacement. $V_e = \frac{\pi}{4} \times b^2 \times s \times n$ where b is bore, s is stroke, and n is number of cylinders.	m^3
C	Coefficients, e.g. C_1, C_2, C_3, \dots	
\dot{V}_t	Theoretical volumetric fresh mixture flow rate	m^3/s
A	Cross section area	m^2
ρ	Fluid density.	kg/m^3
p	Fluid pressure. p_0 is stagnation pressure.	N/m^2
T	Absolute temperature. T_0 is stagnation temperature.	K
v	Fluid speed	m/s
θ	Percent of throttle opening, $0 \leq \theta \leq 1$.	
λ	Stoichiometric air-fuel ratio	
η	Engine efficiency (including thermal and mechanical efficiency)	
E_f	Fuel energy density	j/kg
m'	Molecular mass of gas. For air $m' = 28.9$	$kg/kmol$
R	Universal gas constant. For air $R = 8314.5$	$(N\cdot m)/(kg\cdot mol\cdot K)$
k	Specific heat ratio. For air $k = 1.407$	

II-1. INTRODUCTION

With the rapid development of wireless communication technologies, especially inter-vehicular communications, and the soon-to-be-launched Vehicle Infrastructure Integration (VII) Initiative at the United State Department of Transportation (USDOT), road vehicles will be able to talk with each other as well as with the roadside in the future. Consequently, a new class of in-vehicle applications can be enabled by VII to significantly increase the efficiency and safety of road vehicles. For example, a cooperative driving assistance system (CDAS) can be developed to serve as an ever-vigilant co-pilot constantly watching out for potential hazards and warning

drivers of an imminent danger. If connected to proper actuation devices, such a CDAS can readily lead to a partial or full vehicle automation system.

However, a long way has to go before the promising future becomes true. Among the many difficulties anticipated along the way such as standards, financing, deployment, operations, and management, a technical issue involving engine modeling appears particularly interesting and serves as the focal point of this paper. As mentioned above, a CDAS acts as the key to various VII-enabled in-vehicle applications and central to the CDAS is an algorithm which typically checks potential collisions once every second or even more frequently. An engine model is highly relevant in this picture because one needs to determine a vehicle's ability to accelerate (e.g. to speed up as appropriate or to escape from an imminent collision) with reasonable accuracy and excellent computational efficiency.

Though there has been a wealth of literature in the area of modeling internal combustion engines, these engine models were developed with a special interest in assisting engine design, analysis, control, and diagnosis. While these models are quite successful for their intended purposes, several reasons prevent them from being equally successful in the above VII-enabled in-vehicle applications. For example, a typical procedure in the CDAS is to invoke routines such as car following, lane changing, and gap acceptance logic to check potential collisions. In order to ensure safety, this procedure has to be repeated with such a high frequency that conventional engine models, due to their intrinsic complexity, is beyond the capacity of a contemporary on-board computer. In addition, most of these engine models require proprietary parameters such as throttle body size and mass of piston. This prevents wide deployment of such a CDAS across a wide variety of vehicle platforms. Therefore, special criteria apply to an ideal engine model suited for VII-enabled in-vehicle applications. Most salient of these criteria are the following:

- **Accuracy:** The engine model must provide reasonable accuracy to predict engine performance with throttle and engine speed as inputs and engine power and torque as outputs.
- **Efficiency:** The engine model must be simple enough to facilitate on-board computing with high frequency in real time.
- **Accessibility:** To assist wide deployment across different vehicle platforms, the engine model should not rely on proprietary parameters and variables that are difficult to measure. All the information needed to run the model (such as peak engine power, torque, and their associated engine speeds) should be publicly available (e.g. <http://www.cars.com>).
- **Formulation:** The engine model should be analytical. Engine models based on look-up tables are not only prohibitive to prepare for each individual vehicle but also resource-demanding in computation.
- **Calibration:** The engine model should involve the least calibration effort – no calibration is most desirable. Again, it would be a daunting task if an engine model has to be calibrated for every vehicle.

With the above list of criteria, the objective of this paper is to develop a simple engine model that is suited for VII-enabled in-vehicle applications. Three simple engine models are presented in this paper. These engine models will be formulated and empirically validated. Special attention will be paid to the above criteria when comparing the performance of these models, based on which, the best model will be recommended. Comparing with existing work reviewed in the next section, this paper claims a limited theoretical contribution in that these

models are rather simple and some of the modeling concepts (such as polynomial fitting and the Bernoulli's principle) have already been explored in the past. However, the recommended model does fill a gap in non-conventional arena such as VII-enabled in-vehicle applications where an excellent computational efficiency and reasonable accuracy are desirable.

This paper is arranged as follows. The next section provides a review of existing literature in engine modeling. This is followed by the formulation of three simple engine models including an existing model and two models developed by the authors. These models will be validated using empirical data and their performance will be evaluated. Finally, the paper is summarized and some concluding remarks will be provided.

II-2. REVIEW OF EXISTING ENGINE MODELS

The objective of this section is to highlight existing work in the area of engine modeling. Given the fact that a great deal of literature exists on this topic, it is practically intractable to include all efforts in the history. Nevertheless, the review presented below should provide a brief overview of historical evolution and current status.

It appears that efforts of engine modeling have a much shorter history than the engine itself. The first physically based dynamic engine models were reported in (Sheffi et al. 1982), (Sheffi et al. 1982), (Dobner 1980), (Dobner 1983), and (Coates and Fruechte 1984) which recognized the effects of throttle and intake manifold dynamics. Much of the early efforts in engine modeling has been surveyed in (Sheffi et al. 1982) with a focus on internal combustion engine models for control.

A noticeable trend in engine modeling was characterized by the desire for more modeling details and higher accuracy. For example, many early engine models focused on the modeling of intake manifold dynamics and a direction of improvement was to include more stages and components of the power generating process. Engine models developed in (Moskwa and Hedrick 1987) and (Yoon and Sunwoo 2001) included fuel film dynamics and engine rotational dynamics with transport delays. Continuing on this modeling approach, A three state engine model was developed in (Cho and Hedrick 1989) based on the work in (Dobner 1980) (Dobner 1983) and (Moskwa 1988). In this three state model, the first state equation dealt with intake manifold dynamics, the second state equation concerned with fueling, and the third state equation described the rotational dynamics of the engine. Shortly after, Akinci et al (Akinci et al. 2003) also presented a nonlinear three state dynamic model of an SI engine. These states included air mass flow through the throttle, air mass flow filling the manifold, and air mass flow entering the cylinder. Further effort was reported in (Puleston et al. 2002) where the engine model consisted of an air flow subsystem, a fuelling subsystem, a mechanical subsystem, and an input-output subsystem. Rizzoni (Rizzoni 1989) formulated a global model for the IC engine. The engine is viewed as a system with input given by cylinder pressure and output corresponding to crankshaft angular acceleration and crankshaft torque. The cylinder pressure is deterministically related to net engine torque through the geometry and dynamics of the reciprocating assembly. The relationship between net engine torque and crankshaft angular acceleration is explained in terms

of a passive second-order electrical circuit model with constant parameters. At the same time, Rizzoni (Rizzoni 1989) published another paper on a stochastic model for the cylinder pressure process and the dynamics of the IC engine. Based on a brief description of the above deterministic model, a stochastic model was proposed for the cylinder pressure process. The deterministic model and the stochastic representation were tied together in a Kalman filter model. Crossley and Cook (Crossley and Cook 1991) proposed a nonlinear engine model by representing the throttle body and inlet airflow, engine pumping and torque generation as nonlinear algebraic relations. Hong (Hong 1995) developed an engine model based on the “filling and emptying” method for unsteady gas flow across the engine cylinder (Heywood 1989). The model included equations of mass, momentum, and energy conservation which could be solved for the rate of change in temperature, pressure, and mass in combustion chambers. In their low-dimensional, physically motivated engine model, Dawdy and Matalas (Dawdy and Matalas 1964) tried to capture the interaction between stochastic, small-scale fluctuations in engine parameters and nonlinear deterministic coupling between successive engine cycles. The model also considered the fact that residual cylinder gas from each cycle alters the in-cylinder fuel-air ratio and thus the combustion efficiency in succeeding cycles. Recognizing that the assumption of constant mass moments of inertia had led many engine models to poor performance under high engine speed, Shiao et al (Shiao et al. 1994) proposed two approaches to address this issue. One approach was based on the Newtonian method and the other uses the Lagrangian method to derive the nonlinear governing equations for internal combustion engine kinematics and dynamic forces. To serve the purpose of engine design of internal combustion engine, the engine model in (Chiavola 2001) was able to describe the unsteady gas flow in both intake and exhaust systems and analyzing the behavior of air-fuel flow in complex geometry. As an attempt to capture even more details, Ma and Perkins (Ma and Perkins 2003) developed a complicated engine model involving twelve degrees of freedom. The model consisted of equations of motion for the major components in an internal combustion engine using a recursive formulation. Components included are the engine block, pistons, connecting rods, crankshaft, balance shafts, main bearings, and engine mounts.

At the applied side, efforts were identified which made use of existing engine models or further existing work. In their research on the slip control through controlling the angle of the throttle valve, Kabgarian and Kazemi (Kabgarian and Kazemi 2001) applied the two-state engine model developed in (Cho and Hedrick 1989). Toward the development of a nonlinear model-based control strategy for hybrid vehicles, Wagner et al (Wagner et al. 2003) developed a real-time engine model very similar to the engine model in (Moskwa and Hedrick 1987). In their effort on hybrid vehicle modeling, Delprat et al (Delprat et al. 2004) adopted a model to describe the dynamic behavior of the IC engine torque. The details of this model, however, were missing and a reference to a document in a foreign language was provided. Scillieri et al (Scillieri et al. 2005) developed a direct-injection spark-ignition (DISI) engine model to demonstrate the potential performance benefits of reference feedforward control. The model used a polynomial expression to relate engine torque to the fuel flow rate and the cylinder flow rate. A couple of simulation packages containing ICE models were also identified. Butler et al (Butler et al. 1999) described a simulation and modeling package, V-Elph, which includes a built-in ICE model and facilitates in-depth studies of electric vehicle (EV) and hybrid EV (HEV) configurations. Gao et al (Gao et al. 2007) discussed a simulation package ADVISOR which contained an ICE model which was fitted using empirical data obtained from the component testing.

In contrast to the ever-increasing desire for modeling details, some applications such as real-time engine control necessitate simpler engine models. Recognizing the inherently nonlinear nature of internal combustion engines, Cook and Powell (Cook and Powell 1988) argued that a linear engine model might be desirable for the purpose of engine control analysis. In their attempt of a non-thermodynamic modeling approach, they reduced the nonlinear model presented in (Sheffi et al. 1982) to a linear model. Despite the simplification, they showed that linear model was adequate to capture the necessary dynamics for engine control analysis. To facilitate the development of AICC (Autonomous Intelligent Cruise Control), Swaroop et al (Swaroop et al. 1994) used an engine model which was essentially the first state equation developed in (Cho and Hedrick 1989). Based on the ideal gas law, this model expressed the mass air flow rate into the cylinder as the product of four terms. These terms are a constant dependent on the throttle body size, the throttle opening, a pressure influence function, and the ratio of the air pressure to the intake manifold pressure. A very simple engine model was presented in (Grieve 2006) for teaching purpose. This engine model applies Bernoulli's principle at both sides of the throttle and the intake valve without considering choked flow. The resulting power model consists of two terms: a constant term representing the amount of power that would be generated if there were no constriction and a correction term representing the constriction at the throttle and the intake valve. An extremely simple engine model was suggested by Genta (Genta 2003) to assist the modeling of vehicle dynamics. This model used a polynomial to empirically approximate the engine performance curves.

In addition to model complexity and accuracy, one of the frequently concerned metrics is the model accessibility. For example, some models are very accessible because they only require parameters which are publicly available such as peak power, peak torque and their associated engine speeds; some models may require varying number of proprietary parameters (such as throttle body size and mass of piston) or variable which are very difficult to measure (such as intake manifold pressure and temperature). Such a concern is especially relevant in some non-automotive applications such as transportation engineering. To facilitate the comparison of relative merits of the above models in terms of these metrics, a summary table is provided in Appendix A.

II-3. SIMPLE MATHEMATICAL ENGINE MODELS

This section presents three simple engine models. Model I is an existing one and Model II and III are developed by the authors.

II-3.1. Model I: Polynomial Model

In an effort to develop a dynamic vehicle model, (Genta 2003) suggested a very simple engine model that uses a polynomial to empirically approximate the relationship between engine power, P , and engine speed, ω , i.e.

$$P = \sum_{i=1}^3 C_i \omega^i \quad (I-1)$$

where C_i , $i = 0, 1, 2, 3$ are coefficients and can be estimated from empirical engine curves. (Artamonov et al. 1976) suggested the following values for spark ignition engines:

$$C_1 = P_{\max} / \omega_p, \quad C_2 = P_{\max} / \omega_p^2, \quad C_3 = -P_{\max} / \omega_p^3 \quad (\text{I-2})$$

As is well known, engine torque, Γ_e , is engine power divided by engine speed:

$$\Gamma = \sum_{i=1}^3 C_i \omega^{i-1} \quad (\text{I-3})$$

where coefficients C_i , $i = 0, 1, 2, 3$ remain the same as in I-2.

II-3.2. Model II: Parabolic Model

This model uses a parabola to approximate the torque curve:

$$\Gamma = C_1 + C_2 (\omega - \omega_t)^2 \quad (\text{II-1})$$

where C_1 and C_2 are constants. To constrain that the power curve peaks at ω_p , we replace C_1 with a different coefficient C_3 :

$$P = C_3 \omega + C_2 (\omega - \omega_t)^2 \omega \quad (\text{II-2})$$

Knowing that the engine outputs P_{\max} at ω_p and Γ_{\max} at ω_t , we have:

$$\Gamma_{\max} = C_1 + C_2 (\omega_t - \omega_t)^2 = C_1 \quad (\text{II-3})$$

and

$$P_{\max} = C_3 \omega_p + C_2 (\omega_p - \omega_t)^2 \omega_p \quad (\text{II-4})$$

and

$$\left. \frac{dP}{d\omega} \right|_{\omega=\omega_p} = \left(C_3 + C_2 (\omega - \omega_t)^2 + 2C_2 \omega (\omega - \omega_t) \right) \Big|_{\omega=\omega_p} = 0 \quad (\text{II-5})$$

Solve equations II-4 and II-5

$$C_2 = -\frac{P_{\max}}{2\omega_p^2 (\omega_p - \omega_t)} \quad (\text{II-6})$$

$$C_3 = \frac{P_{\max}}{2\omega_p^2} (3\omega_p - \omega_t)$$

Therefore

$$\Gamma = \Gamma_{\max} - \frac{P_{\max}}{2\omega_p^2 (\omega_p - \omega_t)} (\omega - \omega_t)^2 \quad (\text{II-7})$$

and

$$P = \frac{P_{\max}}{2\omega_p^2} (3\omega_p - \omega_t) \omega - \frac{P_{\max}}{2\omega_p^2 (\omega_p - \omega_t)} (\omega - \omega_t)^2 \omega \quad (\text{II-8})$$

Equations II-7 and II-8 constitutes Model II which guarantees that its power and torque curves peak as their respective peak engine speeds.

II-3.3. Model III: Bernoulli Model

This model is based on Bernoulli's principle which states that, for an ideal fluid (e.g. air) on which no external work is performed, an increase in velocity occurs simultaneously with decrease in pressure or a change in the fluid's gravitational potential energy. When the fluid flows through a pipe (e.g. the intake manifold) with a constriction (e.g. the throttle) in it, the fluid velocity at the constriction must increase in order to satisfy the equation of continuity, while its pressure must decrease because of conservation of energy. The limiting condition of this effect is choked flow where the mass flow rate is independent of the downstream pressure (e.g. in the combustion chamber), depending only on the temperature and pressure on the upstream side of the constriction (e.g. the atmosphere). The physical point at which the choking occurs is when the fluid velocity at the constriction is at sonic conditions or at a Mach number (the ratio of fluid velocity and sound speed) of 1. With the above preparation, the Bernoulli engine model is developed as follows.

Theoretical volumetric fresh mixture flow rate into the engine, \dot{V}_t is

$$\dot{V}_t \text{ (m}^3\text{/s)} = V_e \text{ (m}^3\text{/cycle)} \times \text{cycles/rev} \times \text{engine speed (rev/s)} \quad \text{(III-1)}$$

where V_e is engine displacement, $\text{cycles/rev} = 1/2$ for a four-stroke engine, and $\text{engine speed (rev/s)} = \omega_e / 2\pi$ where ω_e is engine speed in rad/s . Therefore,

$$\dot{V}_t = V_e \times \frac{1}{2} \times \frac{\omega}{2\pi} = \frac{V_e \omega_e}{4\pi} \quad \text{(III-2)}$$

This model assumes that the air is an ideal gas. According to ideal gas law:

$$pV = \frac{m}{m'} RT \quad \text{(III-3)}$$

where p is the absolute pressure, V is the volume of the vessel containing the gas, m is the mass of the gas, m' is the molar mass of the gas, R is the gas constant, and T is the temperature in Kelvin. Therefore, $m = \frac{pm'}{RT} V$ and the density of the gas in the vessel is

$$\rho = \frac{m}{V} = \frac{pm'}{RT} = \frac{p}{R_a T} \quad \text{(III-4)}$$

where $R_a = \frac{R}{m'}$ and for air $R_a \approx 287 \text{ Nm/kg/K}$. Further, the mass air flow rate, \dot{m} , as a function of the volumetric air flow rate, \dot{V} is

$$\dot{m} = \frac{pm'}{RT} \dot{V} = \frac{p}{R_a T} \dot{V} \quad \text{(III-5)}$$

In terms of the engine, \dot{V} is replaced by \dot{V}_t and the speed of air flow is $v = \frac{\dot{V}_t}{A}$ where A is the cross section area of any point in the intake manifold. The constriction in the manifold is the throttle whose cross section area is $\theta \times A$ where θ is percent of throttle opening. So the mass flow rate of air entering the engine is

$$\dot{m} = \frac{P}{R_a T} \dot{V}_t = \frac{P}{R_a T} v A \quad (\text{III-6})$$

According to compressible fluid mechanics (Bar-Meir 2007), the speed of air flow, v , is related to a Mach number, M_a , which is the ratio of air flow speed to sound speed $v_s = \sqrt{k R_a T}$, i.e.

$$M_a = \frac{v}{v_s} = \frac{v}{\sqrt{k R_a T}} = \frac{\dot{V}_t}{A \sqrt{k R_a T}} \quad (\text{III-7})$$

where k is specific heat ratio.

Assume stagnation state (where the flow is brought into a complete motionless condition in isentropic process without other forces) holds. Follow the stagnation state for ideal gas model in Sections 4.1 and 4.2 of (Bar-Meir 2007), equation III-6 can be translated to:

$$\dot{m} = A \left(\frac{\sqrt{k} M_a p_0}{\sqrt{R_a T_0}} \right) \left(1 + \frac{k-1}{2} M_a^2 \right)^{-\frac{k+1}{2(k-1)}} \quad (\text{III-8a})$$

where p_0 and T_0 are stagnation pressure and temperature, respectively. Plug (III-7) into (III-8a) gives

$$\dot{m} = A \left(\frac{\dot{V}_t p_0}{A R_a T_0} \right) \left(1 + \frac{\dot{V}_t^2 (k-1)}{2 A^2 k R_a T_0} \right)^{-\frac{k+1}{2(k-1)}} \quad (\text{III-8b})$$

Notice that equations III-8a and III-8b apply to flow everywhere. When the flow is choked (i.e. $M_a = 1$) and stagnation conditions (i.e. temperature, pressure) do not change, equation (III-8a) reduces to:

$$\dot{m} = A \left(\frac{\sqrt{k} p_0}{\sqrt{R_a T_0}} \right) \left(1 + \frac{k-1}{2} \right)^{-\frac{k+1}{2(k-1)}} \quad (\text{III-9})$$

Similar to Model II, assume exact Stoichiometric air-fuel ratio λ , fuel energy density E_f , engine thermal efficiency η , the power developed by the engine is:

$$P = \eta_e E_f \lambda \left[A \left(\frac{\dot{V}_t p_0}{A R_a T_0} \right) \left(1 + \frac{\dot{V}_t^2 (k-1)}{2 A^2 k R_a T_0} \right)^{-\frac{k+1}{2(k-1)}} \right] \quad (\text{III-10})$$

Plug in equation III-2,

$$P = \eta_e E_f \lambda \left[A \left(\frac{V_e \omega_e p_0}{4 \pi A R_a T_0} \right) \left(1 + \frac{V_e^2 \omega_e^2 (k-1)}{32 \pi^2 A^2 k R_a T_0} \right)^{-\frac{k+1}{2(k-1)}} \right] \quad (\text{III-11})$$

The torque that the engine develops is

$$\Gamma = \eta_e E_f \lambda \left[A \left(\frac{V_e P_0}{4\pi A R_a T_0} \right) \left(1 + \frac{V_e^2 \omega_e^2 (k-1)}{32\pi^2 A^2 k R_a T_0} \right)^{\frac{k+1}{2(k-1)}} \right] \quad (\text{III-12})$$

Empirical comparison shows that this model explains engine performance quite well up to peak torque and power. However, there exhibits considerable differences between the model and empirical engine curves after peak torque and power. Therefore, the engine model is modified by adding a correction term:

$$P = \eta_e E_f \lambda \left[A \left(\frac{V_e \omega_e P_0}{4\pi A R_a T_0} \right) \left(1 + \frac{V_e^2 \omega_e^2 (k-1)}{32\pi^2 A^2 k R_a T_0} \right)^{\frac{k+1}{2(k-1)}} \right] - \alpha P_{\max} e^{-\frac{\beta(\omega - \omega_p)}{\omega_p}} \quad (\text{III-13})$$

where α and β are coefficients to be calibrated.

It should be pointed out that the idea of this Bernoulli's principle-based model is not new and similar discussion can be found in existing work such as (Ehsani et al. 2005).

II-4. VALIDATION AND COMPARISON OF THE ENGINE MODELS

To validate the three engine models as well as to compare their relative performance, we need empirical engine power and torque curves. Unfortunately, we do not have much choice because such empirical data are typically proprietary unless they are made available by interested parties. Provided in this validation study are empirical curves of the following four automotive engines: 2008 Mercedes CLS, 2006 Honda Civic, 2006 Pagani Zonda, and 1964 Chevrolet Corvair. These engines may establish a good presence of vehicle makes, models, and model years. Listed in Table II-1 are technical specifications of these engines. Values for other parameters in the three models are provided in Appendix.

Table II-1 Technical specifications of engines used in the validation study

Engine	2008 Mercedes CLS	2006 Honda Civic	2006 Pagani Zonda	1964 Chevrolet Corvair
Tech Spec				
Peak power (kW)	286	103	408	84
ω at peak power (rpm)	6000	6300	5900	4400
Peak Torque (Nm)	531	174	750	209
ω at peak torque (rpm)	4000	4300	4050	2800
Engine displacement (liter)	5.46	1.80	7.30	2.68
Compression ratio	10.7 : 1	10.5 : 1	10 : 1	9.25 : 1
Throttle body diameter (mm)	50 *	60	80 *	58

* values are estimated

The primary criterion to evaluate these models is accuracy. The following figures illustrate the relative performance of the three models using the empirical engine data as a benchmark. Each figure pertains to one of the engines and consists of two subplots – one for power and the other for torque. In principle, the torque curve should contain the same information as the power curve because power is simply the product of torque and engine speed. However, many empirical engine curves showed slight differences between the power and the torque, so both of them are incorporated here to facilitate comparison. Noticeably, these figures consistently suggest that model II performs the best among the three and model III performs the better than model I.

In Figure II-1, model II fits the empirical power curve very well. Model III also fits well except peak power. Model I meets the peak power but over estimates the remaining part of the empirical curve. In terms of torque, model II meets the peak torque but generally falls under the empirical curve. Model III would give a better fit if it were shifted slightly to the left. Model I generally deviates from the empirical curve by shifting to the left translating upward.

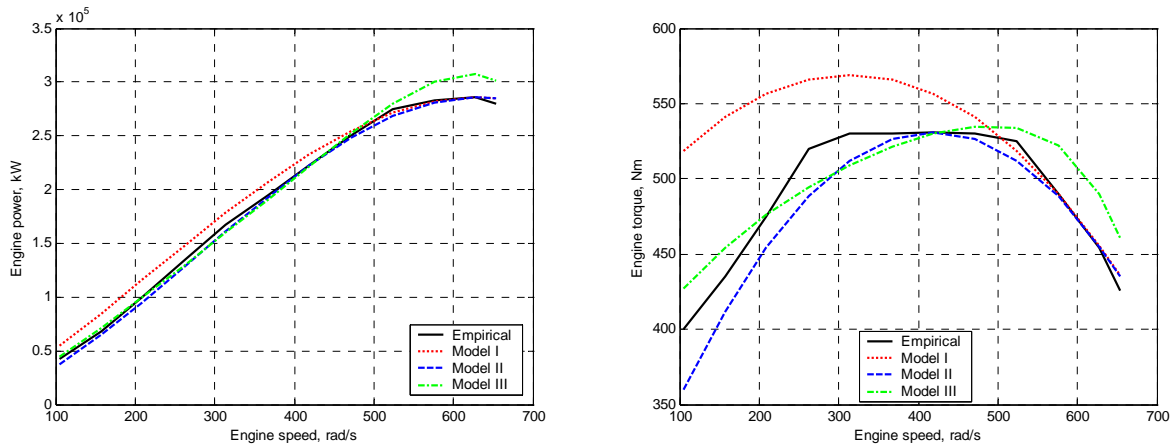


Figure II-1 Comparison of the three models based on 2008 Mercedes CLS engine

Figure II-2 generally shows about the same pattern as that in Figure II-1 with more noticeable deviations of the models I and III. Though model II agrees with the peak torque, the model does not fit the empirical torque curve well under very low and very high engine speeds.

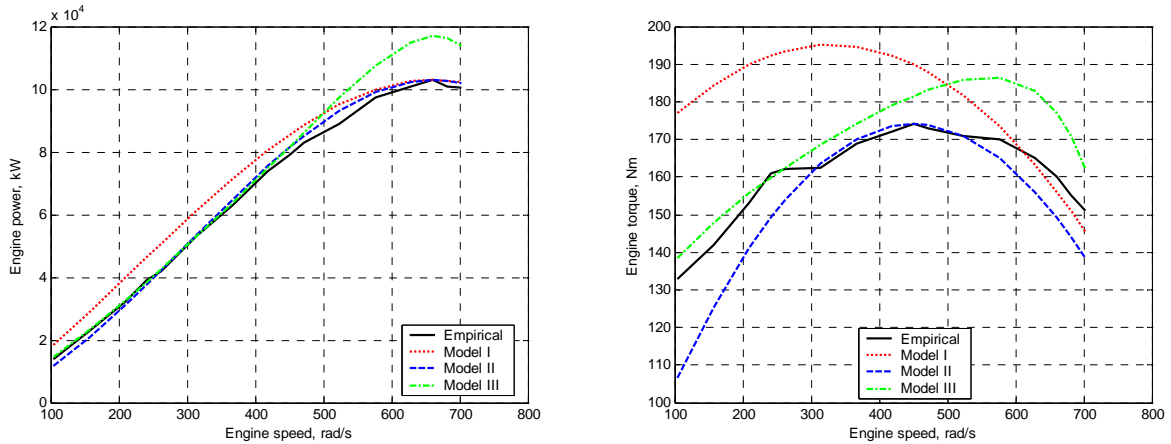


Figure II-2 Comparison of the three models based on 2006 Honda Civic engine

In Figure II-3, model II generally fit the empirical curves well except for the depressed parts under low to middle engine speeds. Model III's torque curve drops too fast after the peak torque. Model I increasingly deviates from the empirical curves as engine speed decreases.

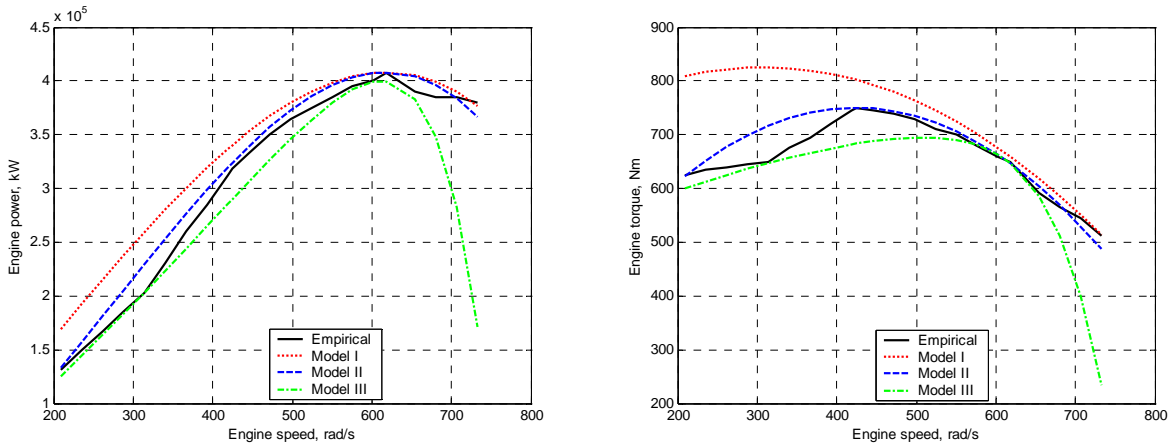


Figure II-3 Comparison of the three models based on 2006 Pagani Zonda engine

In Figure II-4, Model II generally over estimates the torque before the peak torque. Except for a good fit of the peak torque, model I and III generally over estimate the torque.

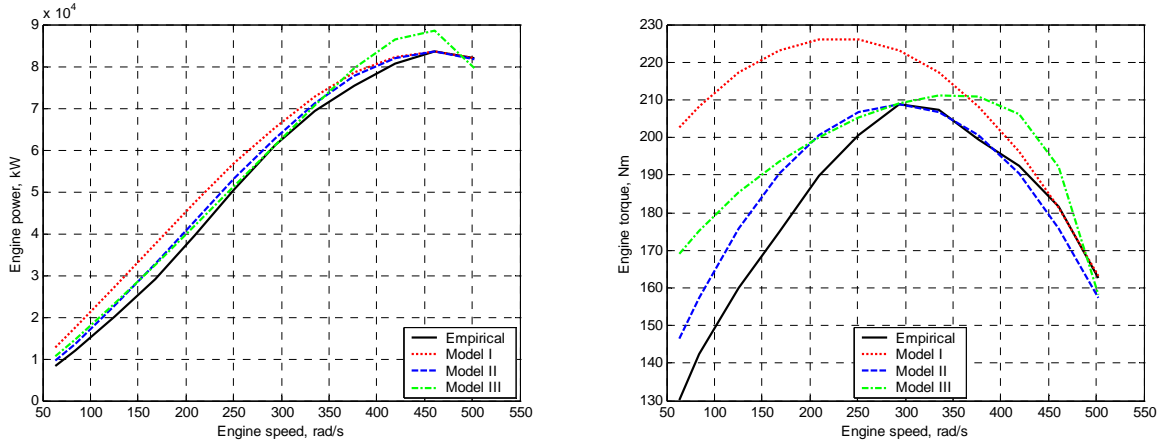


Figure II-4 Comparison of the three models based on 1964 Chevrolet Corvair engine

In order to quantify the performance of the three models, we use mean absolute percentage error (MAPE) as the measure of effectiveness. MAPE is calculated as:

$$MAPE = \frac{1}{n} \sum_{i=1}^n \frac{Y_i - X_i}{Y_i}$$

where n is number of samples, X_i is model estimate, and Y_i is the corresponding empirical value.

Figure II-5 confirms that Model II performs consistently well in both power and torque across the four engines. Its MAPE generally ranges between 3-7%. Though less than model II, Model III generally performs quite well too and its MAPE ranges between 4-9%. Model I performs the least in the three and its MAPE can be as high as 18%.

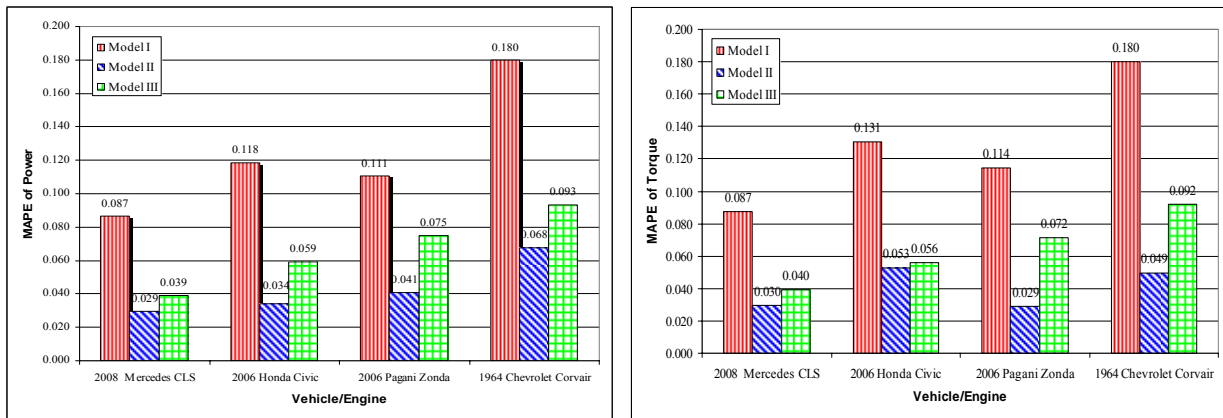


Figure II-5 Performance of the three models (left: MAPE of power, right: MAPE of torque)

The second criterion to evaluate these models is accessibility, i.e. the involvement of proprietary parameters and difficult-to-measure variables. In this regard, Model I and II are excellent because all they need are peak power and torque and their associated engine speeds. Such information is readily available on the Internet. Model III requires the throttle body diameter, a proprietary parameter which is less desirable. The third criterion to evaluate is

computational efficiency / complexity. On average, model I and II consume about 3.2×10^{-5} CPU time, while model III takes 0.075 CPU time. Though these numbers appear negligible, their difference is pronounced in real time applications or applications involving thousands of vehicles/engines, both of which are typical applications in transportation. In terms of the fourth criterion – formulation, the three models are all analytical. The fifth criterion of evaluation is calibration effort. In this regard, model I and II involves virtually no calibration – all they need are peak power and torque and their associated engine speeds. Model III involves some calibration due to its proprietary parameter and calibration coefficients. The above comparison results are listed in Appendix A. In summary, Model II appears to be the best choice among the three in terms of all the evaluation criteria.

II-5. CONCLUSION

Taking the perspective of transportation engineering, this paper aims at developing an appropriate engine model suited for transportation applications. Due to the nature of transportation where large numbers of vehicles/engines are typically involved, some special criteria apply to such an engine model. The foremost of these criteria are reasonable accuracy, computational efficiency, and model accessibility. Three simple engine models are presented in this paper: model I is an existing model and model II and III are developed by the authors. These models are formulated, validated, and evaluated. In terms of accuracy, model II and III are moderate while model I is low. In terms of efficiency, the three models are all acceptable with model I and II being particularly efficient. In terms of accessibility, model I and II are excellent because they do not require any proprietary parameter or difficult-to-measure variable. Overall, model II appears the best choice among the three in terms of all the evaluation criteria.

II-6. APPENDIX

A. A high-level comparison of engine models

Engine model	Complexity /Efficiency	Accuracy	Access-ibility	Proprietary parameters / difficult-to-measure variables	Intended applications
Model I (Genta 2003)	low	low	high	none	Vehicle dynamics
Model II	low	moderate	high	none	Transportation
Model III	moderate	moderate	moderate	Intake manifold diameter	Vehicle dynamics
(Grieve 2006)	low	low	moderate	Intake manifold diameter and intake valve opening	Vehicle dynamics
(Swaroop et al. 1994)	low	moderate	low	throttle body diameter, pressure influence function, intake manifold pressure	Autonomous Cruise Control

(Cook and Powell 1988)	moderate	moderate	low	manifold pressure, function of manifold pressure and speed	Engine control analysis
(Sheffi et al. 1982), (Sheffi et al. 1982), (Dobner 1980), (Dobner 1983)	moderate	moderate	low	throttle body diameter, pressure influence function, intake manifold pressure	Engine control analysis
(Moskwa and Hedrick 1987) and (Yoon and Sunwoo 2001)	high	high	low	throttle body diameter, throttle shaft diameter, engine inertia, volume of intake manifold and surge tank, angle for minimum leakage area, intake manifold pressure, cylinder pressure, engine coolant temperature, crank angle, fraction of injected fuel entering into the film	engine control algorithms
(Cho and Hedrick 1989)	high	high	N/A	N/A	powertrain controllers and dynamics
(Akinci et al. 2003)	high	high	low	discharge coefficient, throttle body diameter, volume of manifold, manifold pressure, manifold temperature	Electric throttle control algorithm
(Puleston et al. 2002)	high	high	low	engine inertia, throttle open area, manifold volume, spark advance, manifold pressure	air-fuel ratio control and speed control
(Shiao et al. 1994)	high	high	low	mass of piston, mass and length of connecting rod, mass of crankshaft, piston offset, cylinder pressure force	engine diagnostics and control
(Chiavola 2001)	high	high	low	duct diameter, Connecting rod length, Inlet valve diameter, Exhaust valve diameter, Exhaust valve opening, Exhaust valve closing	the design procedure of internal combustion engines
(Ma and Perkins 2003)	Very high	high	low	crankshaft deformation mode shapes, mass matrix of the engine system, stiffness and damping coefficients of the	up-front design of engines for noise and

				bearing, fluid viscosity, journal radius, journal clearance, Euler angles of the engine block with respect to the vehicle body, strain tensor, relative displacement between the crankshaft and the engine block	vibration targets.
--	--	--	--	--	--------------------

B. Values for parameters in the three engine models

Engine efficiency $\eta = 0.29$

Fuel energy density $E_f = 46900000 \text{ j/kg}$

Stoichiometric air-fuel ratio $\lambda = 0.068$

Air density $\rho = 1.29 \text{ kg/m}^3$

Atmospheric pressure $p = 101325 \text{ Pa}$

$\pi = 3.14159$

Heat capacity ratio of ideal gas $k = 1.407$

Molar mass of air $m' = 28.9$

Universal gas constant $R = 8314.5 \text{ (N}\cdot\text{m)/(kgmol}\cdot\text{K)}$

Coefficients in Model III: $\alpha = 0.15$ and $\beta = 10$

REFERENCES

- Akinci, B., C. Hendrickson and I. Karaesmen (2003). Exploiting Motor Vehicle Information and Communications Technology for Transportation Engineering. *Journal of Transportation Engineering* 129(5): pp. 469-474.
- Artamonov, M. D., V. A. Ilarionov and M. M. Morin (1976). *Motor Vehicles : Fundamentals and Design*, Mir Publishers, Moscow
- Bar-Meir, G. (2007). *Fundamentals of Compressible Fluid Mechanics*, Version 0.4.4.2a, Potto Project.
- Butler, K. L., M. Ehsani and P. Kamath (1999). Matlab-based modeling and simulation package for electric and hybrid electric vehicle design. *IEEE Transactions on Vehicular Technology* 48(6): 1770-1778.
- Chiavola, O. (2001). Integrated modelling of internal combustion engine intake and exhaust systems. *Proceedings of the Institution of Mechanical Engineers, Part A: Journal of Power and Energy* 215(4): 495-506.
- Cho, D. and J. K. Hedrick (1989). Automotive powertrain modeling for control. *Journal of Dynamic Systems, Measurement and Control, Transactions ASME* 111(4): 568-576.
- Coates, F. E. and R. D. Fruechte (1984). *Dynamic Engine Models for Control Development. Part II: Application to Idle Speed Control*. *International Journal of Vehicle Design Special Publication(SP4)*: 75.
- Cook, J. A. and B. K. Powell (1988). Modeling of an Internal Combustion Engine for Control Analysis. *IEEE Control Systems Magazine*: 20-26.
- Crossley, P. R. and J. A. Cook (1991). *A Nonlinear Engine Model for Drivetrain System Development*, Institute of Electrical and Electronics Engineers.
- Dawdy, D. R. and N. C. Matalas (1964). *Statistical and probability analysis of hydrologic data, part III: Analysis of variance, covariance and time series*, New York, McGraw-Hill Book Company.
- Delprat, S., J. Lauber, T. M. Guerra and J. Rimaux (2004). Control of a parallel hybrid powertrain: Optimal control. *IEEE Transactions on Vehicular Technology* 53(3): 872-881.
- Dobner, D. J. (1980) *A Mathematical Engine Model for Development of Dynamic Engine Control*. Society of Automotive Engineers (SAE) Report No. 800054.
- Dobner, D. J. (1983). *Dynamic Engine Models for Control Development. Part I: Nonlinear and Linear Model Formulation*. *International Journal of Vehicle Design Technological Advances in Vehicle Design Series(SP4)*: 54-74.
- Ehsani, M., Y. M. Gao, S. E. Gay and A. Emadi (2005). *Modern Electric, Hybrid Electric, and Fuel Cell Vehicles*, CRC Press, pp 61-70.
- Gao, D. W., C. Mi and A. Emadi (2007). Modeling and simulation of electric and hybrid vehicles. *Proceedings of the IEEE* 95(4): pp. 729-745.
- Genta, G. (2003). *Motor Vehicle Dynamics: Modeling and Simulation*, World Scientific.
- Grieve, D. J. *Simulation of Dynamic Systems - MECH 337*.
<http://www.tech.plym.ac.uk/sme/mech331/partb1.htm>. Dec. 20, 2006.
- Heywood, J. B. (1989). *Internal combustion engine fundamentals*, McGraw-Hill, New York.
- Hong, C.-W. (1995). Automotive dynamic performance simulator for vehicular powertrain system design. *International Journal of Vehicle Design* 16(2-3): 264-281.

- Kabganian, M. and R. Kazemi (2001). A new strategy for traction control in turning via engine modeling. *IEEE Transactions on Vehicular Technology* 50(6): 1540-1548.
- Ma, Z.-D. and N. C. Perkins (2003). An efficient multibody dynamics model for internal combustion engine systems. *Multibody System Dynamics* 10(4): 363-391.
- Moskwa, J. J. (1988). *Automotive Engine Modeling for Real Time Control*. Mechanical Engineering. Cambridge, Massachusetts Institute of Technology. Doctor of Philosophy: 241.
- Moskwa, J. J. and J. K. Hedrick (1987). *Automotive engine modeling for real time control application*, Minneapolis, MN, USA, American Automatic Control Council, Green Valley, AZ, USA.
- Puleston, P. F., G. Monsees and S. K. Spurgeon (2002). Air-fuel ratio and speed control for low emission vehicles based on sliding mode techniques. *Proceedings of the Institution of Mechanical Engineers. Part I: Journal of Systems and Control Engineering* 216(2): 117-124.
- Rizzoni, G. (1989). Estimate of indicated torque from crankshaft speed fluctuations: A model for the dynamics of the IC engine. *IEEE Transactions on Vehicular Technology* 38(3): 168-179.
- Rizzoni, G. (1989). Stochastic model for the indicated pressure process and the dynamics of the internal combustion engine. *IEEE Transactions on Vehicular Technology* 38(3): 180-192.
- Scillieri, J. J., J. H. Buckland and J. S. Freudenberg (2005). Reference feedforward in the idle speed control of a direct-injection spark-ignition engine. *IEEE Transactions on Vehicular Technology* 54(1): 51-61.
- Sheffi, Y., H. Mahmassani and W. B. Powell (1982). Transportation Network Evacuation Model. *Transportation Research* 16A(3): 209-218.
- Shiao, Y., C.-h. Pan and J. J. Moskwa (1994). Advanced dynamic spark ignition engine modelling for diagnostics and control. *International Journal of Vehicle Design* 15(6): 578-596.
- Swaroop, D., J. K. Hedrick, C. C. Chien and P. Ioannou (1994). Comparison of spacing and headway control laws for automatically controlled vehicles. *Vehicle System Dynamics* 23(8): 597-625.
- Wagner, J. R., D. M. Dawson and L. Zeyu (2003). Nonlinear air-to-fuel ratio and engine speed control for hybrid vehicles. *IEEE Transactions on Vehicular Technology* 52(1): 184-195.
- Yoon, P. and M. Sunwoo (2001). A nonlinear dynamic modelling of SI engines for controller design. *International Journal of Vehicle Design* 26(2-3): 277-297.

Part III

Implementation of Vehicle Powertrain Model in Matlab Simulink

This part presents the implementation of a vehicle powertrain model by combining models presented in the previous two parts. The implementation uses Matlab Simulink as a tool to build the powertrain model which represents vehicle as a feedback control system. The system involves the modeling of fuel supply, energy conversion, power generation, torque transmission, driving force production, acceleration performance, speed regulation, and feedback control. The powertrain model is calibrated and validated using information publicly available online. The results show that the model is capable of capture vehicle acceleration performance with reasonable accuracy.

III-1. MODELING VEHICLE DRIVE CHAIN

Vehicle longitudinal movement can be captured by the modeling of a vehicle's drive chain. This section presents the model of vehicle drive chain by combining the simple vehicle and engine models presented in Part I and II.

III-1.1. Forces Acting on a Vehicle

Force produced by the engine

The engine model that will be incorporated in the DIV model was adapted from the model presented in [48]. This model manages to successfully represent the complexity of the inner working of an internal combustion engine in a very simple and straight forward manner. At the base of this model uses an analytical approach which looks at interaction at between the gas pedal and the force produced by the engine body.

The essence of this approach is that when the driver applies pressure to the gas pedal, the orientation of the throttle valve changes. The change in orientation determines the amount of air flowing into the inlet manifold. The fuel injector then release fuel in a quantity that corresponds to the amount of air flowing through the inlet manifold. This combination of air and fuel is then passed into the cylinders of the engine block, which then combusts, due to a spark from the spark plug. This combustion produces a force on the crankshaft, which then *flows* through the power-train of the vehicle causing the wheel of the vehicle to turn. Figure III-1 provides an illustration of the principle of the engine model developed in [48].

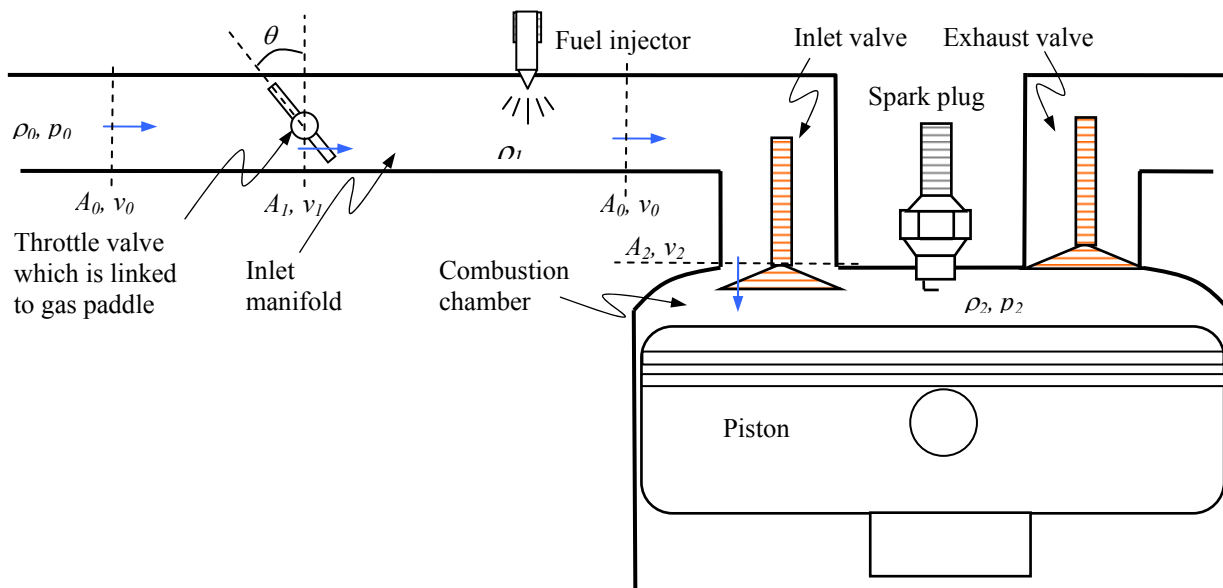


Figure III-1 - Key Components of an Engine's Fuel Injector System

From the above mentioned approach, the key to replicating how an engine works to produce a force that propels a vehicle forward is the amount of fuel being injected in the engine block. But in order to determine the amount of fuel being inject to amount of air flowing in the inlet valve must first be determined. The mass of air flowing into the engine's cylinders, m_a , is equal to the following:

$$m_a = \rho_2 \cdot V_a$$

where:

- ρ_2 - density of the air in the combustion chamber
- V_a - Total volume of the air in the combustion chamber of the engine

However ρ_2 and V_a need to be calculate first. The volume of air in all the combustion chambers of the engine, V_a , is essentially the product of the engine's displacement / volume and its speed; resulting in:

$$V_a = V_e \cdot \frac{1}{2} \cdot \frac{\omega}{2\pi}$$

where:

- V_e - engine displacement (m³)
- ω - engine speed (rad/s)

As for the density of air is the combustion chamber, ρ_2 , it was calculated based on the Bernoulli's Principle which, in essence states that an increase in the speed of a fluid results in a decrease in the pressure or gravitational energy experience by that fluid as long as there no work being done on the fluid. In calculating ρ_2 the cross-sectional areas of the inlet manifold and the opened throttle along with their respective air pressure and densities were used. Therefore after several iterations:

$$\rho_2 = \rho_0 - \frac{\rho_0^2 V_a^2}{2 A_0^2 p_0} \left(\frac{1}{\theta} + \frac{A_0^2}{A_2^2} - 2 \right)$$

where:

- A_0 - cross-sectional area of the inlet manifold (m²)
- A_2 - cross-sectional area of the inlet valve (m²)
- ρ_0 - density of air flow before the throttle (kg/ m³)
- p_0 - air pressure before the throttle (N/ m²)
- θ - throttle position (percent of throttle opening)

After computing the mass of air being taken into to the engine block the corresponding amount of fuel maybe estimated using the Stoichiometric air-fuel ratio (λ) for gasoline, which is 6.8% (fuel by weight). Having a value for the amount of fuel entering the engine, the amount of power that maybe generated by this quantity of fuel can be determined by using the energy fuel density of gasoline, E_f , which is 46.9 MJ/kg. It is known that the efficiency of an internal combustion engine, η , is not 100% and as a result corresponding calculations have to take this fact into account. The effective power, P_{eff} , the power that will be delivered to the vehicle's powertrain mechanism is defined as:

$$P_{eff} = \eta \lambda E_f m_a$$

With the effective calculated the effective torque, P_{eff} , delivered to the wheels of the vehicle can be determined with the following relationship.

$$T_{eff} = \frac{P_{eff}}{\omega}$$

And from the effective torque being delivered to the wheel, the effective force, F_e , produce by the engine to promote vehicle motion can therefore be calculated with the aid of the appropriate final transmission gear ratio, N_{ft} , and wheel radius, r .

$$F_e = \frac{T_{eff} \cdot N_{ft}}{r}$$

Putting everything together, the driving force produced by the engine is:

$$F_e = \frac{N_{ft} \eta \lambda E_f V_e}{4 \pi r} \left[\rho_0 - \frac{\rho_0^2 V_a^2}{2 A_0^2 p_0} \left(\frac{1}{\theta} + \frac{A_0^2}{A_2^2} - 2 \right) \right]$$

The above sections provide a summary of the engine model proposed in [48]. For more details regarding the development of the engine model being incorporated in the DIV model, they can be had by referring to the aforementioned citation. Figure III-2 provides a graphical representation of the basis of the aforementioned engine model to be incorporated in the model.

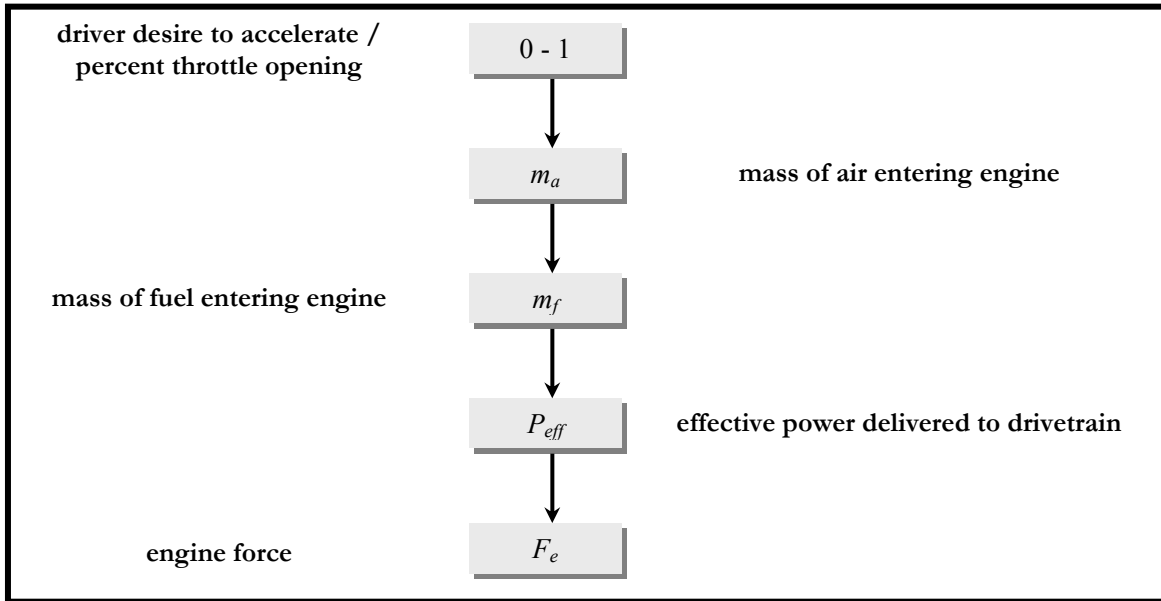


Figure III-2 - Principle behind the engine force and the corresponding driver interaction

Force due to Aerodynamic Drag

Aerodynamic drag is another force that serves to retard the motion of a motor vehicle. This force is dependent of on atmospheric conditions, the frontal area of the vehicle and the velocity of at which the vehicle is traveling relative to the wind. The equation below further describes how the factors affect the aerodynamic drag:

$$R_a = \frac{\rho}{2} C_D A_f V_r^2$$

Where:

ρ	=	Mass density of the air (0.07651 lb/ft ³ - performance test condition)
C_D	=	Coefficient of aerodynamic resistance
A_f	=	Frontal area of the vehicle
V_r	=	Speed of the vehicle relative to the wind.

Net force acting on a vehicle

If one ignores road resistance, grade resistance, rolling resistances, the net force acting on the vehicle can be obtained by combining the above driver force and air dynamic drag:

$$\sum F = F_e - R_a = \frac{N_{ft} \eta \lambda E_f V_e}{4\pi r} \left[\rho_0 - \frac{\rho_0^2 V_a^2}{2 A_0^2 p_0} \left(\frac{1}{\theta} + \frac{A_0^2}{A_2^2} - 2 \right) \right] - \frac{\rho}{2} C_D A_f V_r^2$$

III-1.2. Vehicle Acceleration Performance

Vehicle acceleration, \ddot{x} , can be obtained by Newton's second law of motion:

$$\ddot{x} = \frac{\sum F}{M}$$

Where M is the vehicles equivalent mass which can be approximated by

$$M = n_w \left(\frac{I}{r^2} + m \right) + M_0$$

Where m is the mass of a wheel, n_w number of wheels on the vehicle, I the moment of inertia of each wheel, and M_0 the mass of the vehicle mass after subtracting the mass of the wheels.

With the above acceleration, the vehicle's speed can be determined by integrating the acceleration, and the integration of speed gives the vehicle's displacement:

$$\dot{x} = \int_0^t \ddot{x} \quad \text{and} \quad x = \int_0^t \dot{x}$$

Engine speed

Engine omega, ω , can be determined from vehicle speed, \dot{x} , by considering wheel radius, r , and gear ratio, N_{ft} :

$$\text{Engine omega: } \omega = N_{ft} \frac{\dot{x}}{r} \text{ in rad/s or}$$

$$\text{Engine rpm: } \omega' = \frac{60}{2\pi} N_{ft} \frac{\dot{x}}{r} \text{ in rpm}$$

The engine speed is the necessary input to calculate engine torque production which determines driving force. Driving force determines vehicle acceleration and hence speed. Vehicle speed in return determines engine speed and the loop closes.

III-2. IMPLEMENTATION OF VEHICLE POWERTRAIN

The above vehicle and engine models are implemented using Matlab and a Simulink model of vehicle powertrain is presented below. The implementation uses 2006 Honda Civic as the basis and information regarding the vehicle's specifications is obtained from www.cars.com which is publicly available online.

III-2.1. Data used in the Implementation

Engine data

Engine liters 1.8
 Cylinder configuration I-4
 Engine bore x stroke 3.2" x 3.4"
 Compression ratio 10.50 to 1
 Horsepower 140-hp @ 6,300 rpm
 Torque 128 lbs.-ft. @ 4,300 rpm
 Throttle plate diameter: 45-55 mm (guess)

Transmission data

5-speed automatic w/OD
 Transmission gear ratio (1st) 2.67 (11.45)
 Transmission gear ratio (2nd) 1.53 (6.56)
 Transmission gear ratio (3rd) 1.02 (4.38)
 Transmission gear ratio (4th) .72 (3.09)
 Transmission gear ratio (5th) .53 (2.27)
 Transmission gear ratio (reverse) 1.96

Powertrain data

Axle ratio 4.29
Axle ratio : 4.44 Optional
Front-wheel drive Standard

Vehicle weight and dimension

Curb weight 2,685 lbs. (1217.9 kg)
Towing capacity 1,000 lbs.
Exterior length 176.7"
Exterior body width 69.0"
Exterior height 56.5"
Wheelbase 106.3"
Wheel size 16" (0.4064 m)
Front tread 59.0"
Rear tread 60.2"
Turning radius 17.7'

Vehicle performance

0-60 mph 7.92 seconds
1/4 mile 16.14 seconds at 89.57 mph
Lateral acceleration .82 g
Slalom 60 mph

General information

for gasoline spark ignition (SI) internal combustion engine (ICE):

Engine efficiency $\eta = 0.29$

Fuel energy density $E_f = 46900000 \text{ j/kg}$

Stoichiometric air-fuel ratio $\lambda = 0.068$

Air density $\rho = 1.29 \text{ kg/m}^3$

Atmospheric pressure $p = 101325 \text{ Pa}$

$\pi = 3.14159$

Heat capacity ratio of ideal gas $k = 1.407$

Molar mass of air $m' = 28.9$

Universal gas constant $R = 8314.5 \text{ (N}\cdot\text{m)/(kgmol}\cdot\text{K)}$

Coefficients in Model III: $\alpha = 0.15$ and $\beta = 10$

III-2.2. Simulink Powertrain Model Description

The implemented Simulink model is presented in Figure III-3.

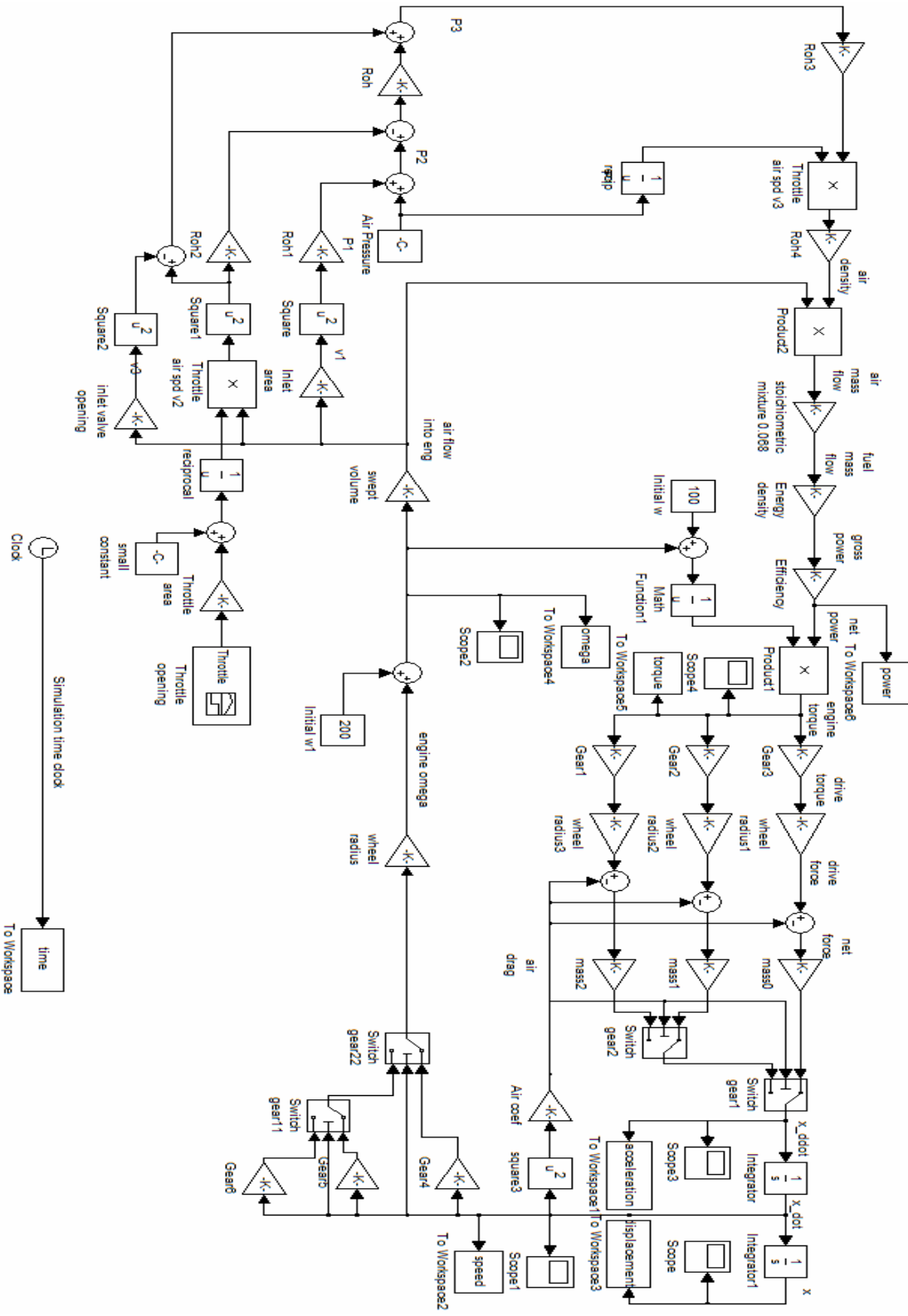


Figure III-3 Simulink model of powertrain

The Simulink powertrain model works as follows:

Starting from block “Product 1” in the middle of the top row,
Engine torque is fed into three gears: “gear1”, “gear2”, and “gear3”.
Engine torque multiplied by overall gear ratio gives drive torque.
Drive torque divided by wheel radius yields drive force.
At the summation point, drive force less air drag yields net force.
Net force divided by vehicle equivalent mass gives vehicle acceleration.
Two switches are used to choose a branch among the three gears.
The selection between the 1st and 2nd gears is mediated by a criterion “speed \geq threshold”.
The output and the 3rd gear is again mediated by another switch.
The output of this switch is the desired acceleration dependent on current gear or vehicle speed.
Integrating acceleration gives vehicle speed.
Integrating speed gives vehicle displacement.
Vehicle speed squared and multiplied by a coefficient yields air drag.
Air drag is the feedback to calculate net force acting on the vehicle.

Vehicle speed multiplied by overall gear ratio is then fed through two switches.
The switches jointly determine the right branch to pass through.
Dividing the amplified speed by wheel radius gives engine omega.
Engine power divided by engine omega gives engine torque
To avoid divide by zero, a small constant is added to the engine omega.

Engine omega times engine swept volume gives volumetric air flow sucked into the engine.
This air flow can be used to determine three speeds:

Air speed in the inlet manifold: $v_1 = \text{air flow} / \text{area of inlet manifold}$

Air speed at the throttle: $v_2 = \text{air flow} / \text{area at the throttle}$

Air speed at the inlet valve: $v_3 = \text{air flow} / \text{area at the inlet valve}$

Note, the area at the throttle is the product of throttle plate area times throttle opening (θ) which is linked to the gas paddle (accelerator).

Assume air pressure in the inlet manifold before the throttle is atmospheric pressure, P_1 .

Apply Bernoulli's principle at the throttle, air pressure after the throttle, P_2 , can be determined.

Apply Bernoulli's principle again at the inlet valve, air pressure in the combustion chamber, P_3 , can be determined.

Proportion air density to air pressure, the density of air in the combustion chamber, ρ_3 , can be determined.

ρ_3 times volumetric air flow gives mass air flow into the engine.

Fuel mass flow can be determined from mass air flow based on stoichiometric mixture.

Fuel mass flow times fuel energy density yields gross power generated by the engine.

Gross engine power times engine efficiency gives net engine power.

Engine power divided by engine speed yields engine torque.

This goes back to the beginning of the model description and this closes the loop.

III-2.3. Simulink Powertrain Model Outputs

The simulation assumes that the vehicle starts at stopped position. When the simulation starts, the driver steps on the gas paddle and open the throttle to full position in 1 second. Outputs of the powertrain model are displaced below.

Figure III-4 shows vehicle acceleration performance. The vehicle starts with a large initial acceleration which quickly drops and then gradually reduces to zero eventually.

Figure III-5 illustrates vehicle speed as a function of time. According to vehicle specifications, the vehicle accelerates from 0 to 60 mph (26.8 m/s) in 7.92 seconds. The model predicts that the process takes about 10 seconds. This is not too bad considering that the model involves many simplifications.

Figure III-6 shoes engine speed, from which the effect of changing gears can be clearly identified.

Figure III-7 shows the vehicle's displacement as a function of time. According to vehicle specifications, the vehicle covers 1/4 mile (402 m) in 16.14 seconds at which time the vehicle speed is 89.57 mph (40 m/s). The Simulink predicts that it takes 17.9 seconds for the vehicle to traverse 1/4 mile and the speed at that moment reaches 87.5 mph (39.1 m/s).

Figure III-8 shows the engine's performance. According to vehicle specifications, the engine's peak horsepower is 140-hp @ 6,300 rpm (104.4 kW @ 660 rad/s) and peak torque is 128 lbs.-ft. @ 4,300 rpm (173.5 Nm @ 450 rad/s). The Simulink predicts the following: peak horsepower 180-hp @ 11765 rmp (134.2 kW @ 1232 rad/s) and peak torque 96.3 lbs.-ft. @ 5061 rpm (130.5 Nm @ 530 rad/s).

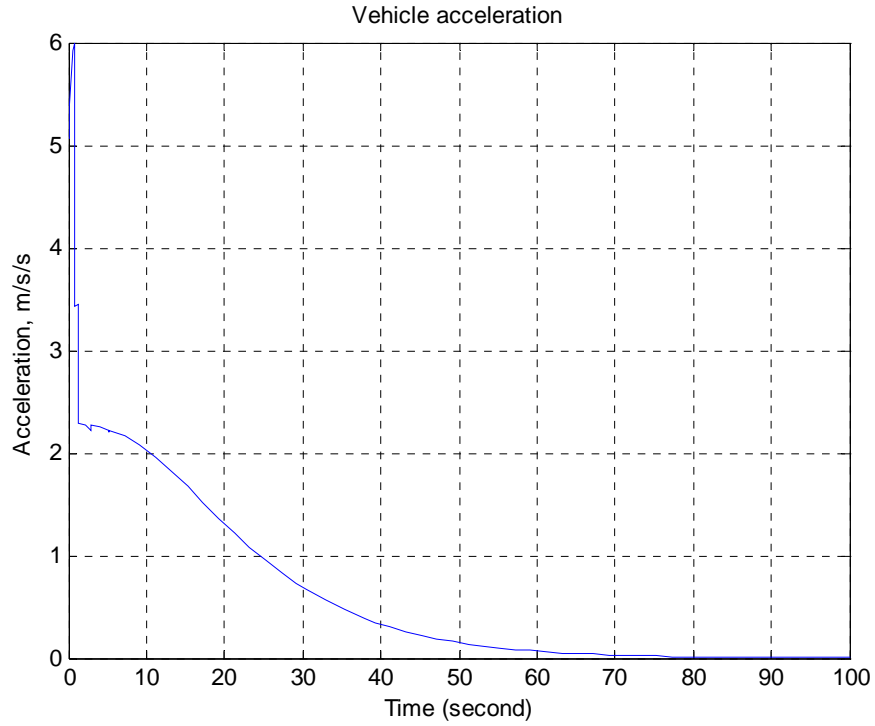


Figure III-4 Vehicle acceleration

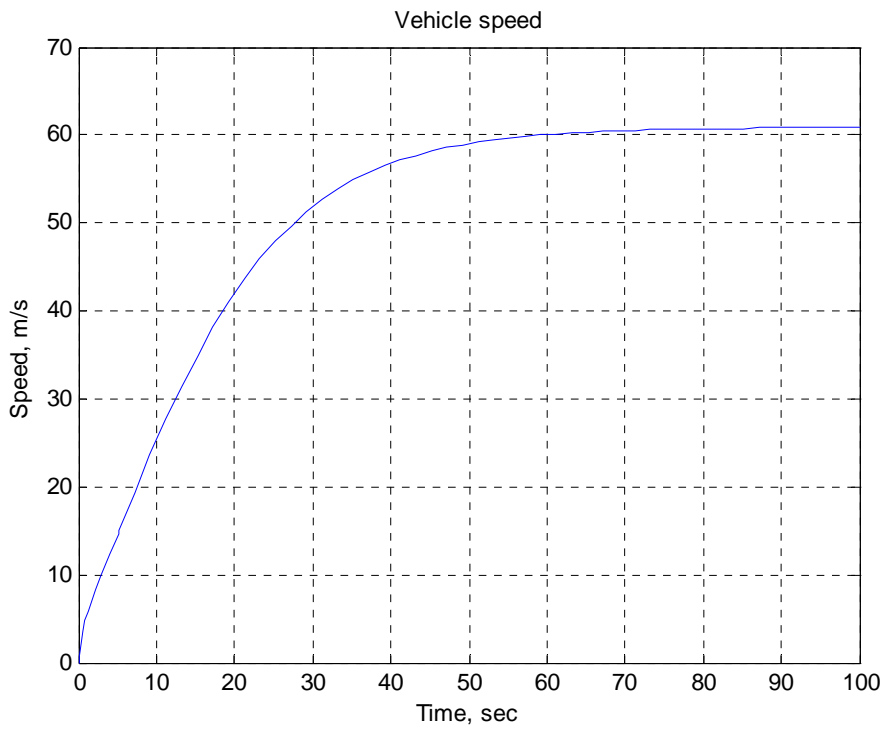


Figure III-5 Vehicle speed

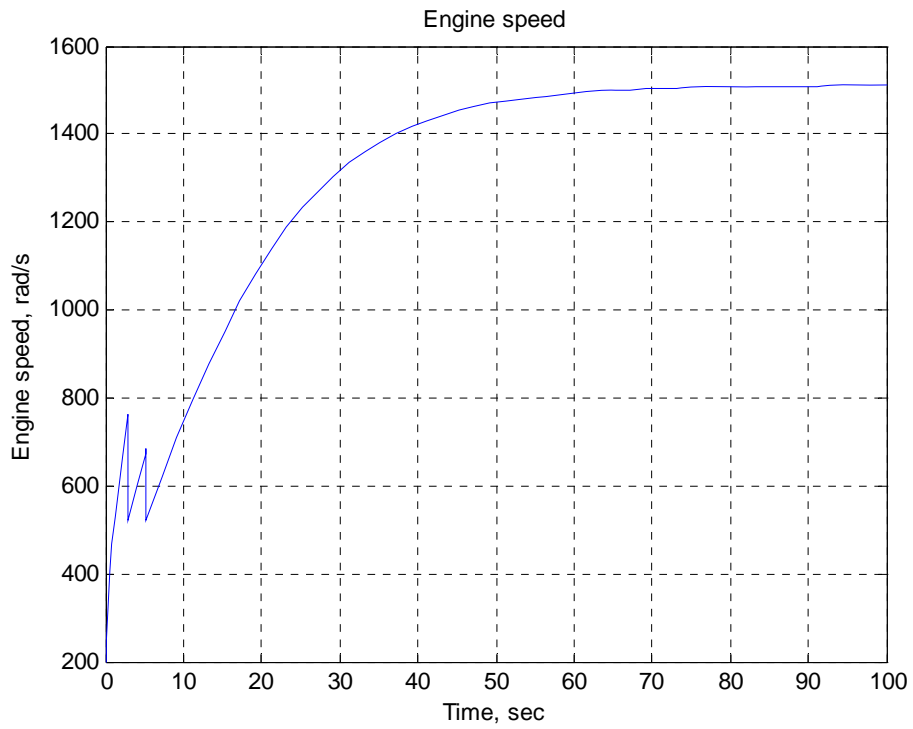


Figure III-6 Engine speed

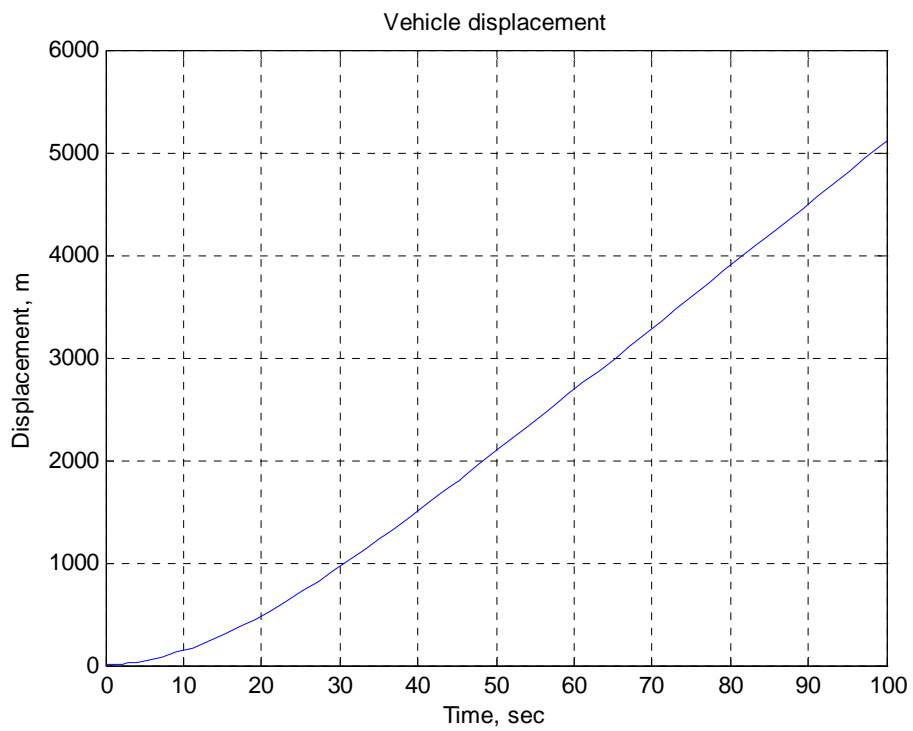


Figure III-7 Vehicle displacement

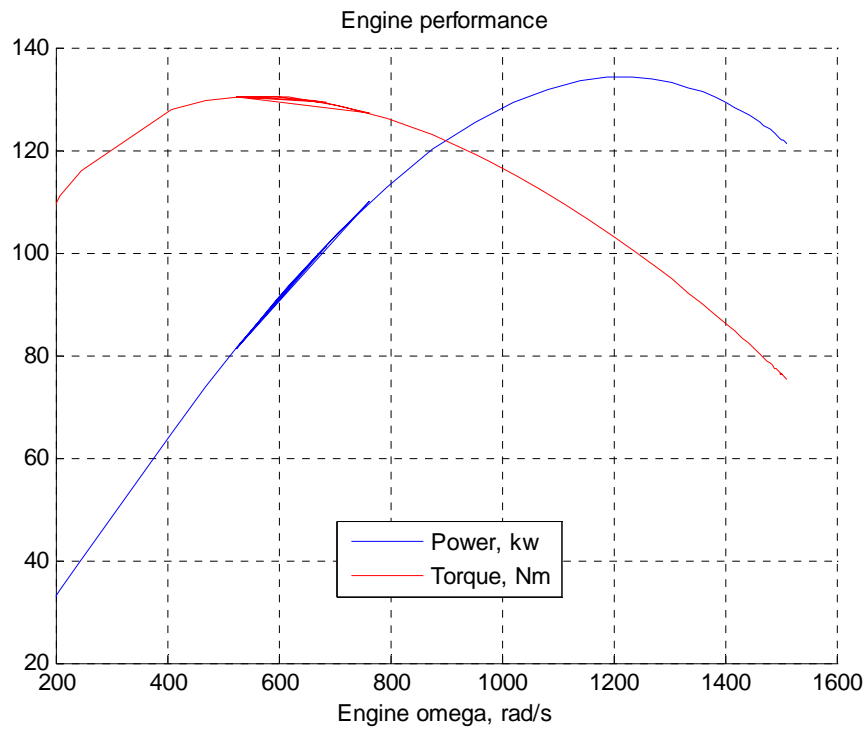


Figure III-8 Engine performance